

Cenozoic drainage reversal on the southern margin of the Colorado Plateau, east-central Arizona, USA

Andre R. Potochnik ^{a,*}, James E. Faulds ^b, Stephen J. Reynolds ^a

^a School of Earth and Space Exploration, Arizona State University, Tempe, AZ 85287, United States of America

^b Nevada Bureau of Mines and Geology, University of Nevada, Reno, NV 89557, United States of America

ARTICLE INFO

Keywords:
Tectonic inversion
Basin and Range
Little Colorado River
Spillover
Salt River

ABSTRACT

Laramide northeast-flowing streams from the ancestral Mogollon highland beveled gently northeast-dipping Late Proterozoic to Cretaceous strata across the southern Colorado Plateau Transition Zone. Late Eocene renewed uplift rejuvenated northeast-flowing streams incising paleocanyons. Apache paleocanyon was incised into the Mogollon highland, including the north-trending Laramide Apache uplift bounded by major reverse faults/monoclines. The Mogollon Rim sequence aggraded in Apache paleocanyon and on a broad alluvial plain to the east. Middle Cenozoic tectonic subsidence of the Transition Zone, aridification, and volcanism combined to aggrade Apache paleocanyon with sedimentary and volcanic rocks from 37.6 to 18.63 Ma. Emplacement of the Mogollon-Datil caldera complex and Chuska erg on the southeastern Colorado Plateau forced streamflow to northwest-dispersal of fluvio-eolian sediment from 34 to 26 Ma. Following erosion by northwest-flowing streams on the southern Colorado Plateau from ~26 to 16 Ma, lake sediments of the lower Bidahochi Fm were deposited. Southwestward reactivation of Laramide faults was underway by ~25 Ma coeval with extensive 25 to 20 Ma Natahes Plateau basalt flows and extreme crustal thinning southwest of the Transition Zone. As northeastward streamflow gradually diminished, a Superstition field ash flow tuff ended northeastward flow at 18.63 Ma and was followed by a period of sluggish southwest stream flow and ponding until after ~14.84 Ma. Southwestward structural subsidence and possible spillover from ancestral Lake Hopi on the Colorado Plateau southern margin caused incision of the southwest-directed Dagger Canyon paleovalley after 14.84, which followed the path of the earlier Apache paleocanyon and possibly to the Sespe delta on the California coast before opening of Gulf of California. Structural collapse of the Tonto Basin to the west induced deposition of the Dagger Canyon Conglomerate in the Dagger Canyon paleovalley before the modern Salt River incised all previous deposits and became integrated with the Gila River during the Plio-Pleistocene.

1. Introduction

Cenozoic tectonism involving structural and topographic inversion of the Colorado Plateau and Basin and Range province in eastern Arizona induced a regional drainage reversal (Peirce et al., 1979; Potochnik and Faulds, 1998; Young and Brennan, 1974). Laramide streams once flowed northeastward from the ancestral Mogollon highland, a broad uplifted region south of the Colorado Plateau, toward large basins containing lakes in the Rocky Mountain region (Cather et al., 2008; Young and Hartman, 2011). The regional drainage systems eventually reversed, resulting in the modern southwestward-flowing Colorado River drainage network. Extensional tectonism and structural foun-dering of the Basin and Range province appear to be largely responsible

for this drainage reversal (Lucchitta, 1979; Potochnik, 2001b; Spencer and Reynolds, 1989; Young and Brennan, 1974).

Although regional drainage reversal has been known and accepted for several decades, many aspects of the timing, duration, and driving forces remain poorly understood, as do the geomorphic mechanisms of drainage reversal. For example, temporal constraints on the abatement of northeast-flowing drainage and detailed relations of the drainage response to regional and local tectonism are poorly known. In addition, the timing, duration, and nature of the intervening period between northeast- and southwest-flowing drainage systems has generally not been addressed. Finally, how does the southwest-flowing Salt River establish itself on the landscape? In this paper, we describe and synthesize depositional systems for Cenozoic sedimentary and volcanic

* Corresponding author at: 18 E Juniper Ave, Flagstaff, AZ 86001, United States of America.
E-mail address: andrepotochnik@gmail.com (A.R. Potochnik).

rocks, as well as structural relations that bear directly on these questions in the Transition Zone of east-central Arizona (Fig. 1).

The findings in this paper are based on integrating detailed stratigraphic, structural, and geochronologic analyses across the region (Fig. 2). This synthesis includes: (1) description of Cenozoic stratigraphy within the Transition Zone between Canyon Creek fault and Tonto Basin (Fig. 3); (2) description of Cenozoic stratigraphy in the southern part of the Colorado Plateau between Canyon Creek fault and Mogollon Rim to establish paleogeographic connections from the Transition Zone to the Colorado Plateau (Fig. 1); and, (3) assessment of dispersal and provenance patterns for Cenozoic sedimentary rock units from paleocurrent indicators and clast counts at locations throughout the region. Radioisotopic analyses of key volcanic rocks provide age constraints. The stratigraphy, provenance, and geochronology of these rocks are related to the underlying paleotopography and patterns of dispersal.

These depositional systems interact with a multi-phase movement history of several fault zones that cross the Transition Zone (Faulds, 1986; Potochnik, 1989, 2001b). This report outlines basic structural elements but reserves most of that discussion for a subsequent report. In describing the depositional systems during drainage reversal, we provide a stratigraphic framework for future workers to develop and test hypotheses on drainage evolution of the southern Colorado Plateau

boundary.

2. Regional setting

The Transition Zone of eastern Arizona is a broad region of rugged mountains and deeply incised canyons that share topographic and structural features of the Colorado Plateau and Basin Range provinces (Peirce et al., 1979). This paper addresses the region extending from the Tonto Basin eastward to the White Mountains. To the north, it includes the Mogollon Rim, a south-facing escarpment and regional drainage divide that defines the southern physiographic edge of the Colorado Plateau (Peirce, 1984). The study area includes the Salt River drainage upstream of Lake Roosevelt (Fig. 1). Most new data in this paper are from the region between the Tonto Basin and Canyon Creek fault. This new work is integrated with previous reports of the region from Canyon Creek fault eastward to the border region of New Mexico (Cather et al., 2008; Potochnik, 1989; Potochnik and Faulds, 1998; Witcher et al., 1994).

Canyon Creek (Finnell, 1962, 1966a) and Cherry Creek faults (Berquist et al., 1981; Faulds, 1986, 1989 and references therein) are fault zones that strike N to NNW and reveal an early history as oppositely-facing monoclines. The monoclines bound and define the north-

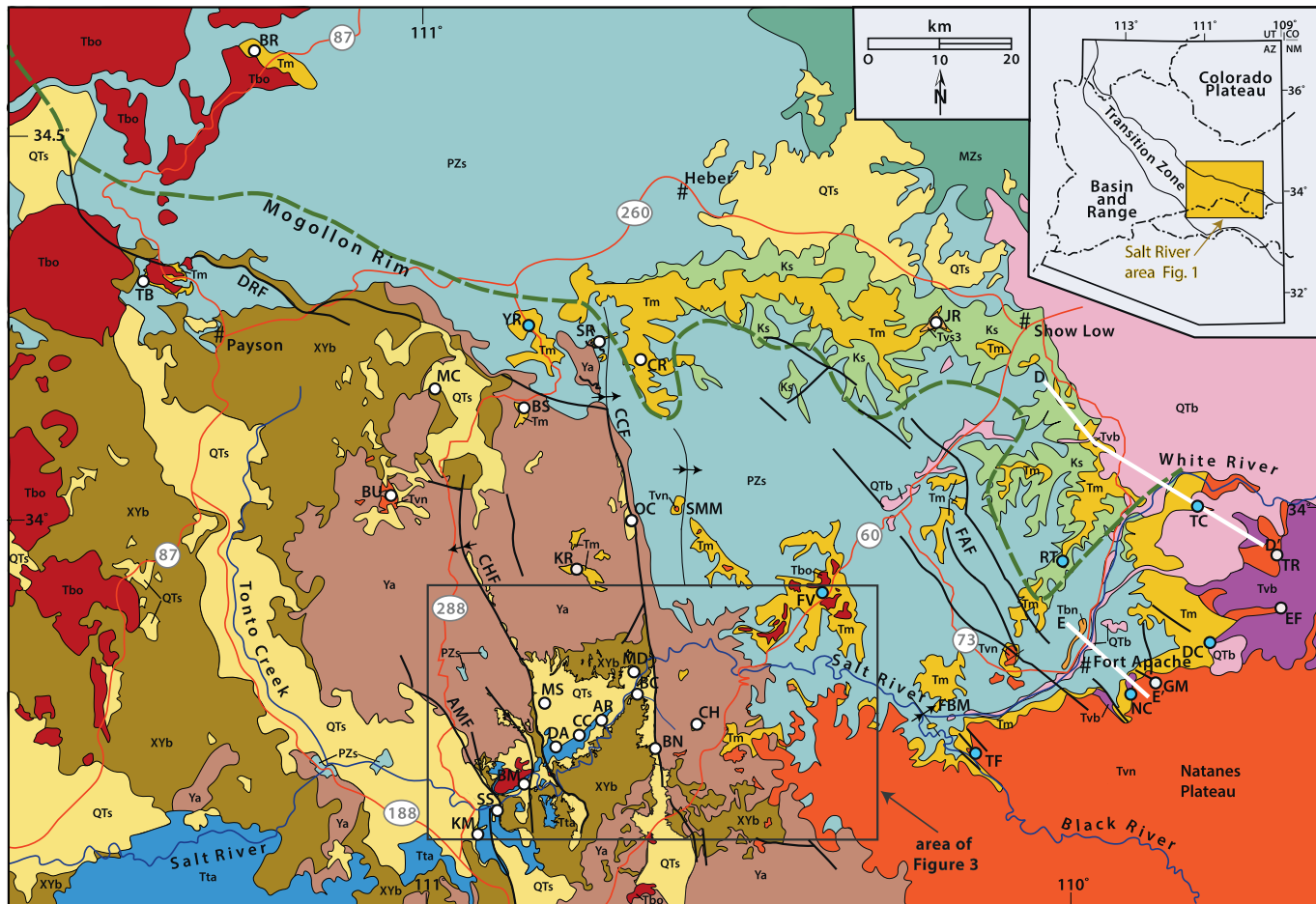


Fig. 1. Geologic map of southern Colorado Plateau-Transition Zone in Salt River region, eastern Arizona. Data collection sites: blue circles after Potochnik, 1989; white circles, this report. Faults and folds: AMF, Armer Mountain fault; CCF, Canyon Creek fault; CHF, Cherry Creek fault; DRF, Diamond Rim fault; FAF, Fort Apache fault zone; FBM, Forks Butte monocline; SMM, Spotted Mountain monocline. Locations: AR, Apache Ridge; BC, Butte Creek; BM, Black Mesa; BN, Bronson Canyon; BR, Blue Ridge; BS, Bottle Spring; BU, Buzzard Roost Mesa; CC, Corral Canyon; CH, Chrysotile; CR, Chediski Ridge; DA, Dagger Canyon; DC, Deep Creek; EF, East Fork of White River; FV, Flying V; GM, Grindstone Mountain; JR, Juniper Ridge; KM, Klondike Mountain; KR, Keystone Ridge; MC, Marsh Creek; MD, Mud Springs Draw; MS, Montague Spring; NC, Nash Canyon; OC, Oak Creek Ranch; RT, Round Top Mtn; SR, Steer Ridge; SS, Shute Spring; TB, Tonto Natural Bridge; TC, Trout Creek; TF, Tick Flat; TR, Tiger Butte; YR, Young Road. Lines of cross sections D, E are shown here. Lines of cross sections A, B, and C are shown in Fig. 3 (area designated here). Lithic designators-colors are shown in Fig. 2 and apply to all subsequent figures unless otherwise noted in caption. Site location symbols apply to all subsequent figures. (For interpretation of the references to color in this figure legend, the reader is referred to the web version of this article.)

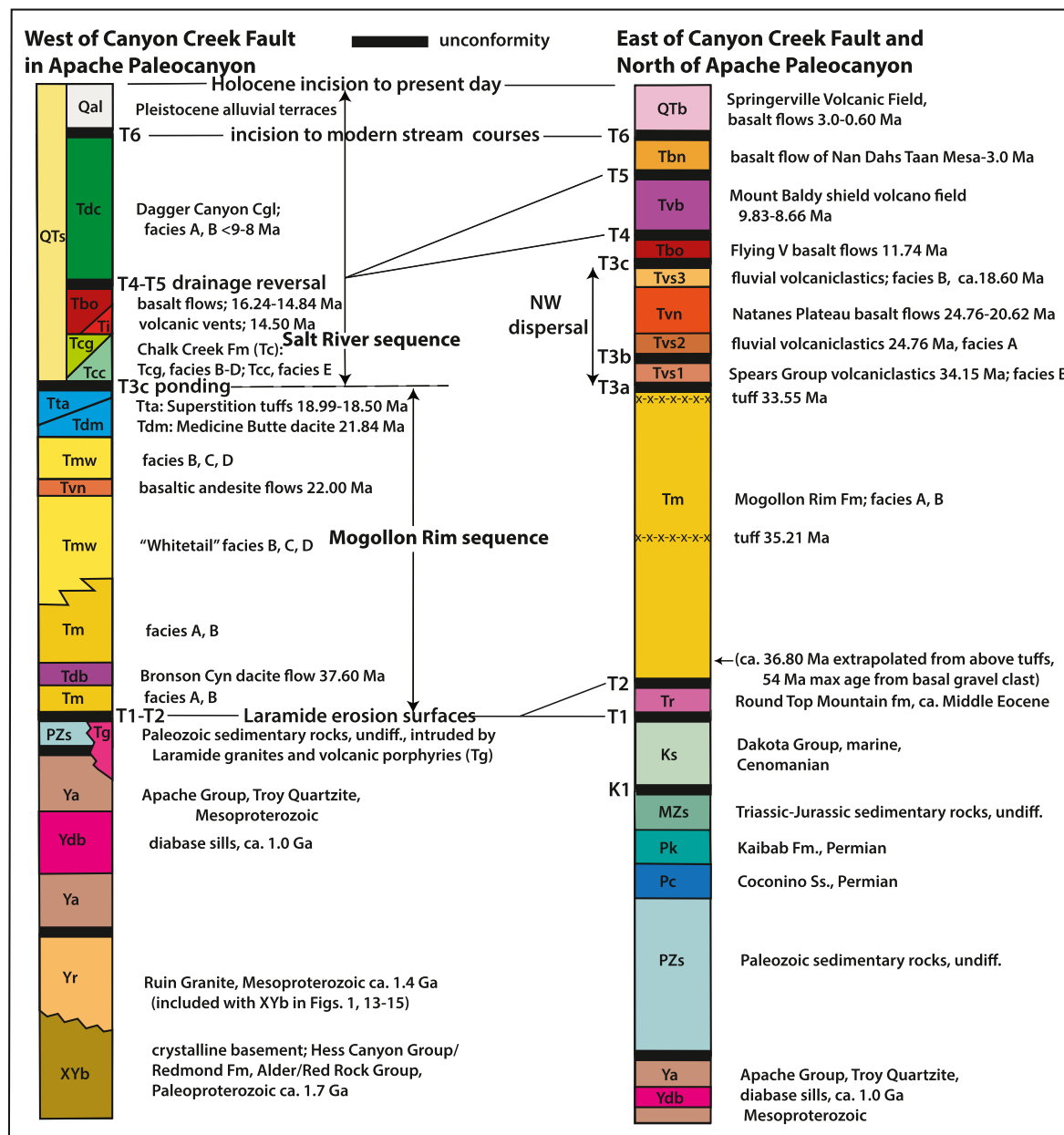


Fig. 2. General stratigraphic columns, Tonto Basin to Mogollon Rim comparing regions southwest and northeast of Canyon Creek fault. Unconformities and stratigraphic units are designated and correlated between columns as discussed in this paper. Vertical thicknesses are generalized. Lithic designators and colors apply to all figures unless noted in caption.

trending Laramide Apache uplift (Davis et al., 1982), an upthrown block ~27 km in width that extends southward from the Mogollon Rim across the Transition Zone (Faulds, 1986; Potochnik and Faulds, 1998 and references therein).

Units within the Transition Zone include Paleozoic and Proterozoic rocks locally overlain by Cenozoic volcanic and sedimentary rocks (Fig. 1). Much of this part of the Transition Zone has extensive exposures of sedimentary rocks of the Mesoproterozoic Apache Group and Troy Quartzite intruded by numerous diabase sills (Schride, 1967; Wrucke, 1989); these rocks regionally dip less than one degree to the northeast (Faulds, 1986). The Apache Group unconformably overlies a thick sequence of steeply tilted Early Proterozoic metasedimentary and metavolcanic rocks (ca. 1700 to 1500 Ma) (Livingston, 1969; Doe et al., 2012) extensively intruded by several generations of Proterozoic granitoids (1650 to 1400 Ma) (Berquist et al., 1981; Wrucke, 1989).

During the Laramide, an east-northeast-trending paleoriver cut

across the Apache uplift (Peirce, 1982), incising a bedrock canyon deeply into pre-Cenozoic rocks (Faulds, 1986, 1989; Potochnik, 2001a, 2001b; Potochnik and Faulds, 1998). This bedrock paleocanyon is here called *Apache paleocanyon* (Fig. 4) to distinguish it from a subsequent nearly coincident – but oppositely-flowing – *Dagger Canyon paleovalley* (Fig. 5) (“proto Salt River” of Anderson et al., 2021) and by the modern Salt River. East of Canyon Creek fault, the Laramide Apache paleocanyon shallows and broadens, merging with widespread outcrops (Fig. 1) of an east-northeast-dispersed alluvial braidplain sequence represented by the Mogollon Rim Formation (Potochnik, 1989). The Mogollon Rim Formation overlies successively younger rocks toward the northeast, from Mesoproterozoic through Lower Permian units within the Transition Zone to Upper Permian through Cretaceous units on the Colorado Plateau (Fig. 1).

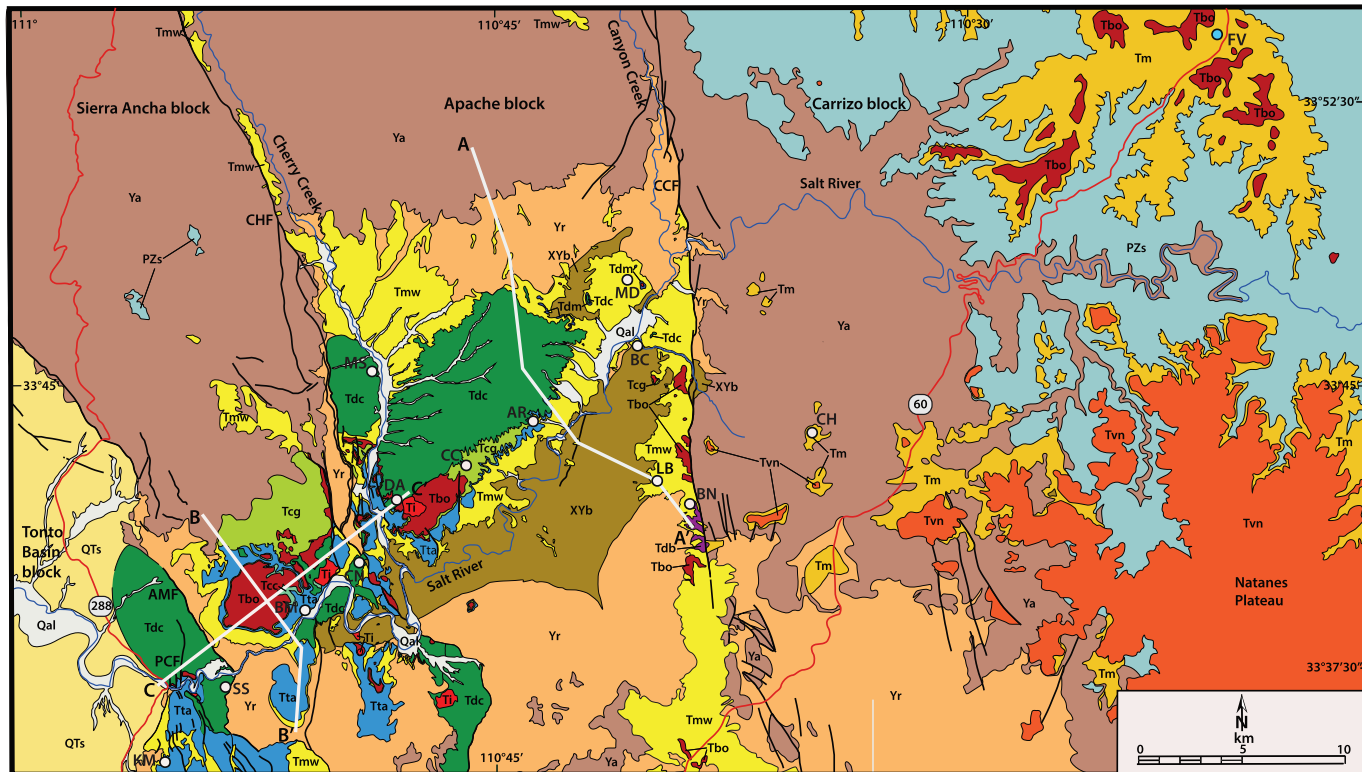
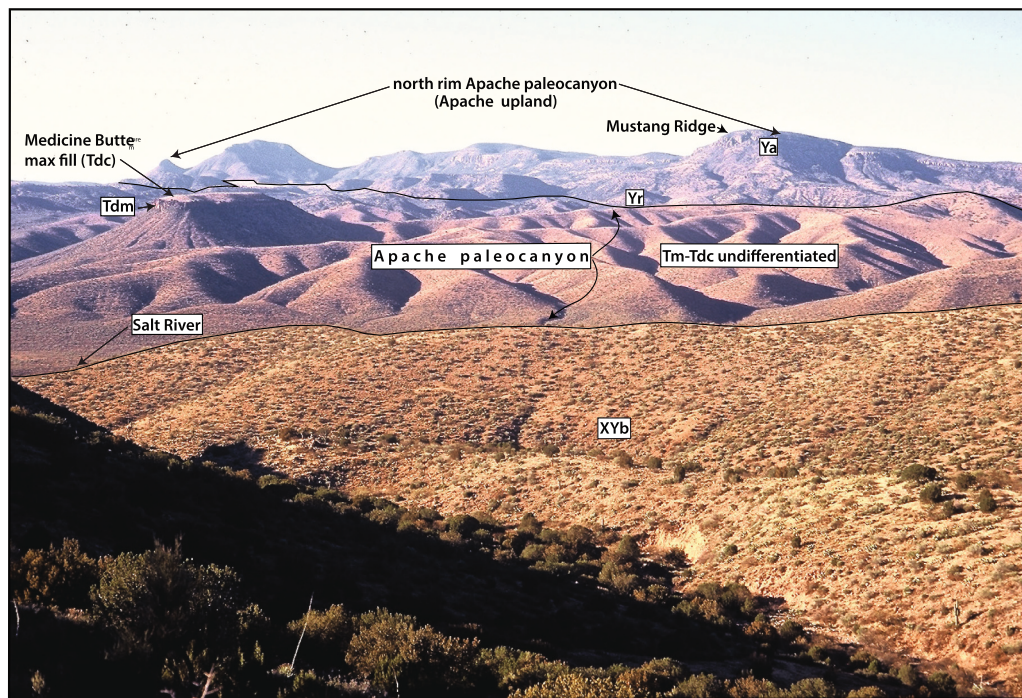


Fig. 3. Geologic map along modern Salt River where it crosses the Laramide Apache uplift and roughly parallels Apache paleocanyon and Dagger Canyon paleovalley. Stratigraphic column locations are shown for Fig. 7. Locations not designated in Fig. 1 are: PCF, Pinal Creek fault; LB, Little Butte. Structural blocks are; Carrizo, Apache, Sierra Ancha, Tonto Basin. Lines of cross sections are shown here as A, B, and C. Area of map is shown in Fig. 1.



3. Previous work

Foundational studies of this region began with Darton's (1925) geologic survey of Arizona in which he included an illustration that shows the large amount of paleotopographic relief in the eastern Arizona

Transition Zone defined by the base of the overlying Cenozoic alluvial units. This paleotopography was subsequently described in abstracts (Peirce, 1982; Davis et al., 1982) followed by the first detailed stratigraphic, structural, and paleogeographic studies of paleocanyon alluvial fill in the vicinity of Cherry Creek fault zone (Faulds, 1986). Faulds

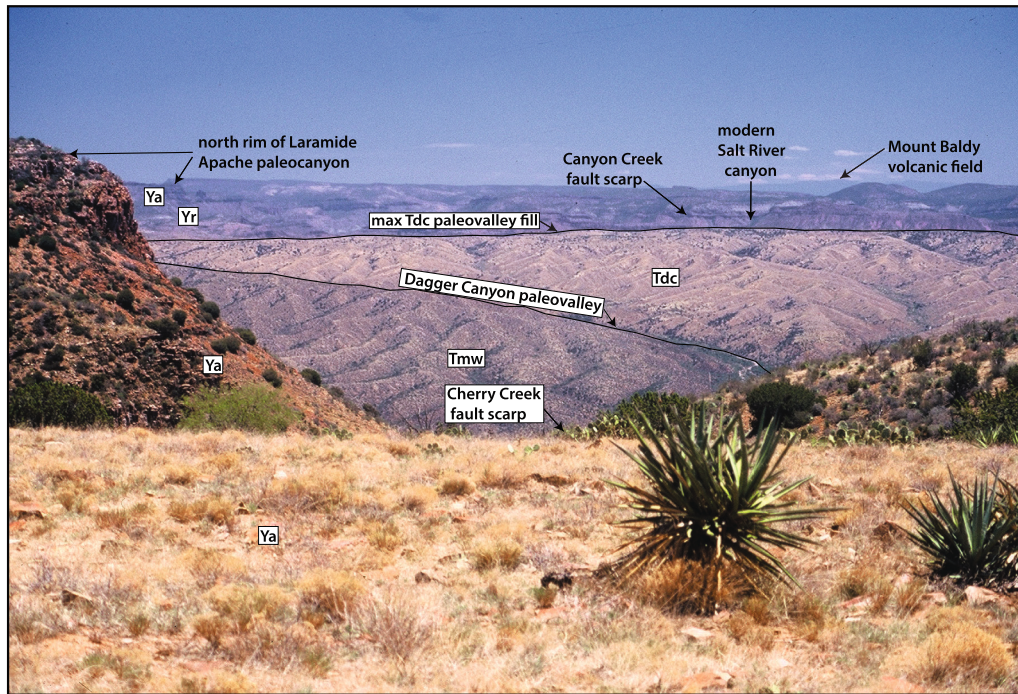


Fig. 5. Photo of view toward NE parallel to axes of Apache paleocanyon and Dagger Canyon paleovalley. View spans Laramide Apache uplift from a vantage point on uplifted late Cenozoic Coon Creek horst (Fig. 17). Note color contrast between northeast transported Whitetail facies of Mogollon Rim sequence (Trmw) and southwest transported Dagger Canyon Conglomerate (Tdc) of Salt River sequence inset within Dagger Canyon paleovalley as a nested formation. (For interpretation of the references to color in this figure legend, the reader is referred to the web version of this article.)

(1986) described a paleocanyon topography (his Salt River paleocanyon) that extended farther to the southwest as part of a much broader uplifted region, commonly referred to as the ancestral Mogollon highland of Laramide age. Faulds (1986) also discussed the implications of other stratigraphic units to the regional drainage reversal, including the 18.6 Ma Apache Leap Tuff and its possible paleogeographic link to the Superstition volcanic field, as well as Miocene lacustrine deposits suggesting a period of internal drainage. A late Laramide alluvial plain sequence east of Canyon Creek fault to the Mogollon Rim was defined and described by Potochnik (1989). Subsequent field work (Potochnik, 2001a) utilized geologic maps (Berquist et al., 1981; Cuffney, 1976; Faulds, 1989; Finnell, 1966a, 1966b; McKay, 1972; Moore and Peirce, 1967; Richard et al., 2000) to describe and establish a contiguous Cenozoic stratigraphic framework from the Mogollon Rim west to the Tonto Basin. The stratigraphic framework was outlined in a preliminary fashion as a field trip guide that described details of the foundational stratigraphic and structural work of this paper (Potochnik and Faulds, 1998). Implications of this work were presented by Potochnik (2001a, 2001b) and are here presented in more refined detail incorporating recent additional work by us and others (Anderson et al., 2021). A detailed geologic map of this part of the Transition Zone included a compilation of this and other previous work along with new geologic mapping (Skotnicki, 2002).

4. Methods

Geologic mapping and field surveys of Cenozoic units were conducted on relevant parts of 63 USGS 7.5 min Quadrangle maps in the study area (Faulds, 1986; Potochnik, 1989; Potochnik, 2001a). In a subset of these maps, mapping was done in sufficient detail to assess contact relations and distribution of stratigraphic units in the most critical areas. Stratigraphic sections across Canyon Creek fault are correlated based on stratigraphy, paleocurrents, age, and provenance. These data collectively allow for correlation of unconformities between sequences of Cenozoic strata, some local and others more regional (Fig. 2). Together, the strata and bounding unconformities allow for a description of drainages and paleogeography across this part of the Transition Zone (Fig. 1). Locations of stratigraphic sections, some faults,

and geographic landmarks are included as a .kmz file in Appendix A. Most radiometric age determinations in the text and figures are listed in Table 1.

5. Results

5.1. Sedimentology and facies

West of Canyon Creek fault, Cenozoic rocks overlie a bedrock surface with hundreds of meters of local paleotopographic relief (Faulds, 1986; Potochnik, 2001b; Potochnik and Faulds, 1998). Cenozoic strata are assigned to one of five facies attributed to alluvial, colluvial, or paludal depositional environments (Fig. 6). Facies are defined according to rounding, sorting, and grain size (maturity) with ancillary consideration of provenance and sedimentary fabrics, such as stratification and imbrication. Lateral and vertical facies changes are commonly observed over 10 m to 100 m distances. Facies A–E in this paper describe progressively more proximal environments of deposition within a paleocanyon setting.

In this paper, facies A and B are interpreted to represent deposits of primary stream systems. Facies A mature gravels are interpreted as main channel deposits, whereas facies B deposits are considered to represent tributary plain/distal alluvial fan deposits. Facies C and D are inferred to be more locally derived units, with facies C consisting of debris flow deposits from tributary canyons and alluvial fans. Facies D deposits are colluvial units, such as those shed from canyon walls and steep mountain fronts. Facies E represents carbonate marsh-shallow lakes, playa, and eolian dune deposits with interfingering alluvial clastics, as occurs in ponded alluvial basins.

Where overlying volcanic flows are not present, these weakly consolidated sedimentary rocks are winnowed of their fine sediment to various degrees. This is particularly pronounced on the southern margin of the Colorado Plateau (Mogollon Rim), where a residual boulder lag gravel is distributed over about 600 km² on this regional drainage divide (Fig. 1) (Finnell, 1966a, 1966b; McKay, 1972; Moore and Peirce, 1967; Peirce, 1984; Potochnik and Faulds, 1998). Such exposures of lag gravel along the southern edge of the Colorado Plateau are commonly called “rim gravels” (Cooley and Davidson, 1963).

Table 1⁴⁰Ar/³⁹Ar ages in this report (informally reported in Potochnik and Faulds, 1998; Potochnik, 2001a)^a.

Sample#	Unit field name	Mineral	Analysis	Age (Ma)	±Error	Lat. N/Long. W	Notes (see Figs. 7, 12)
ARP00-13	Blue Ridge basalt	Groundmass	Plateau	13.70	0.80	34°37.19' / 111°15.49'	Unconformably overlies Tm @BR
ARP00-8	Shendaby dacite plug	Plagioclase	Plateau	14.50	0.30	33°38.08' / 110°49.41'	Intrudes Black Mesa basalt, south of Salt River @BM
WRD-1	Juniper Ridge zircons	Detrital zircon	Laser fusion	18.60	2.70	34°14.99' / 110°12.27'	Tvs3 @JR, Univ. of Arizona Geochron lab
ARP00-5	Apache Leap Tuff	Sanidine	Laser fusion	18.63	0.07	33°45.20' / 110°39.90'	Tta depositional pinchout in Apache paleocanyon
ARP00-2	Black Mesa andesite	Plagioclase	Plateau	22.00	1.80	33°38.56' / 110°52.16'	Intercalated in uppermost Tmw @BM
ARP00-7	Buzzard Roost Mesa flow	Groundmass	Plateau	25.37	0.09	34°01.04' / 111°04.41'	Mafic flow intercalated in QTs @BU
ARP91-3	Blue Ridge tuff	Biotite	Plateau	33.32	0.59	34°37.19' / 111°15.48'	Ash fall tuff in upper Tm section @BR
ARP91-1	Trout Ck ("top tuff")	Biotite	Laser fusion	33.55	0.41	34°00.39' / 109°47.50'	Ash fall tuff in Tm conformably overlain by Tvs1 @TC
ARP91-6	Nash Cyn tuff	Biotite	Laser fusion	34.15	0.60	33°46.94' / 109°54.29'	Ash fall tuff in basal Tvs1 @NC
ARP91-4	Deep Ck ("pink tuff")	Biotite	Laser fusion	35.21	0.40	33°50.82' / 109°46.88'	Correlates with ARP91-2 @TC
ARP91-2	Trout Ck ("7200' tuff")	Biotite	Laser fusion	35.22	0.90	34°01.59' / 109°48.96'	Air fall tuff intercalated midway in Tm type section @TC
ARP00-11	Bronson Cyn rhyodacite	Biotite	Total gas	37.60	0.60	33°41.62' / 110°38.60'	Welded tuff intercalated in lower Tm @BN

Previously reported ages utilized in this report.			Analysis	Age (Ma)	±Error	Reference	
JA18-WRR-1	White River Ridge basalt	Whole rock?	⁴⁰ Ar/ ³⁹ Ar	3.00	0.03	Anderson et al., 2021	Nan Dahs Taan basalt (Tby, this report)
rv88-18a	Bidahochi Fm	Correlation	⁴⁰ Ar/ ³⁹ Ar	6.62	0.05	Dallege et al., 2003	Bidahochi Fm flow, base of member 6
K16-Salt-10	upper Dagger Canyon Cgl	Detrital zircon	⁴⁰ Ar/ ³⁹ Ar	7.15	0.04	Anderson et al., 2021	Detrital maximum age, upper Tdc
980118B	Bidahochi Fm	Plateau	⁴⁰ Ar/ ³⁹ Ar	7.71	0.06	Dallege et al., 2003	Bidahochi Fm tuff, member 4
UA73-79	Tonto Natural Bridge basalt	Whole rock	K-Ar	12.11	0.40	Damon et al., 1996	Basalt flow unconformably overlies Tm @TB
JA18-DC-3	lower Dagger Canyon Cgl.	Detrital sanidine	⁴⁰ Ar/ ³⁹ Ar	12.49	0.04	Anderson et al., 2021	Detrital maximum age, lower Tdc
HB96-1	Bidahochi Fm	Total fusion	⁴⁰ Ar/ ³⁹ Ar	13.71	0.08	Dallege et al., 2003	Bidahochi Fm tuff, member 3
UA83-92	Black Mesa basalt	Whole rock	K-Ar	14.84	0.34	Damon et al., 1996	basalt flow conformably overlies Tcc lakebeds
970616A	Bidahochi Fm	Total fusion	⁴⁰ Ar/ ³⁹ Ar	15.48	0.04	Dallege et al., 2003	basal Bidahochi Fm tuff, member 1
UA75-104	Little Butte basalt flow/neck	Whole rock	K-Ar	16.12	0.39	Damon et al., 1996	Basalt flow overlies Tm @LB
UA83-93	Coon Creek basalt	Whole rock	K-Ar	16.24	0.54	Damon et al., 1996	Basalt flow conformably overlain by Tcc @BM
SH120-2,3	Hackberry Wash tuff	k-Spar	⁴⁰ Ar/ ³⁹ Ar	18.50	0.03	S. Hemmings/W. Holt	Welded Tta overlies Tmw @AR, pers. comm., 2021
SH9-27-19	Cherry Creek tuff	Plagioclase	⁴⁰ Ar/ ³⁹ Ar	18.99	0.07	S. Hemmings/W. Holt	Tuff overlies Tmw north of BM, pers. comm., 2020
UA76-94	Oak Creek Ranch basalt	Whole rock	K-Ar	20.62	1.07	Damon et al., 1996	Basalt flow caps Tm east of OC
UA85-89	Natanes Plateau	Whole rock	K-Ar	21.37	0.49	Damon et al., 1996	Basalt flow overlies Tm east side of CCF near BN
K16-Salt-3	Canyon Creek Butte dacite	Biotite	⁴⁰ Ar/ ³⁹ Ar	21.84	0.03	Anderson et al., 2021	Same as Medicine Butte dacite in this report (Tdm)

^a Radiometric analyses from New Mexico Geochronology Research Laboratory, 1996, 2001.

5.2. Cenozoic stratigraphy west of Canyon Creek fault in Apache paleocanyon

The Cenozoic rocks west of Canyon Creek fault and within Apache paleocanyon are described along a transect that extends northeastward parallel to the axis of the Salt River from Klondike Mountain (directly east of Tonto basin) to Chrysotile. The transect crosses three primary north-striking fault zones; Armer Mountain/Pinal Creek, Cherry Creek, and Canyon Creek faults (Fig. 3).

Stratigraphic columns are hung on the unconformity that marks the drainage reversal. This unconformity separates two distinct packages of rocks – the east-northeast-dispersed *Mogollon Rim sequence* and west-southwest-dispersed units above the unconformity, here referred to as the *Salt River sequence*. The Mogollon Rim and Salt River sequences include intercalated and/or overlying volcanic flows and tuffs (Fig. 7).

Our term "Whitetail facies" is borrowed from the Whitetail Formation (Ransome, 1903), a widely exposed unit in east-central and central

Arizona. South and west of this region, the Whitetail Formation represents a largely pre-volcanic, residual or locally derived unit at the base of Cenozoic sections, where it has been interpreted as infilling and mantling the paleotopography (Ferguson and Trapp, 2001). Previous dates on the Whitetail Formation/Conglomerate range from 33.5 Ma (Krieger et al., 1979) to 20.5 Ma (Ferguson and Trapp, 2001) coeval with the Mogollon Rim sequence as described here. The Whitetail Formation facies interfingers with the Mogollon Rim sequence in this ancestral geomorphic system (Potochnik, 2001a; Potochnik and Faulds, 1998). In these locations of interfingering, it is considered a proximal facies of the Mogollon Rim sequence and is labeled Whitetail facies (Tmw, all figures).

5.3. Mogollon Rim sequence

5.3.1. Mogollon Rim Formation/Whitetail facies stratigraphy

The conglomeratic Mogollon Rim sequence (Tm) is defined by its

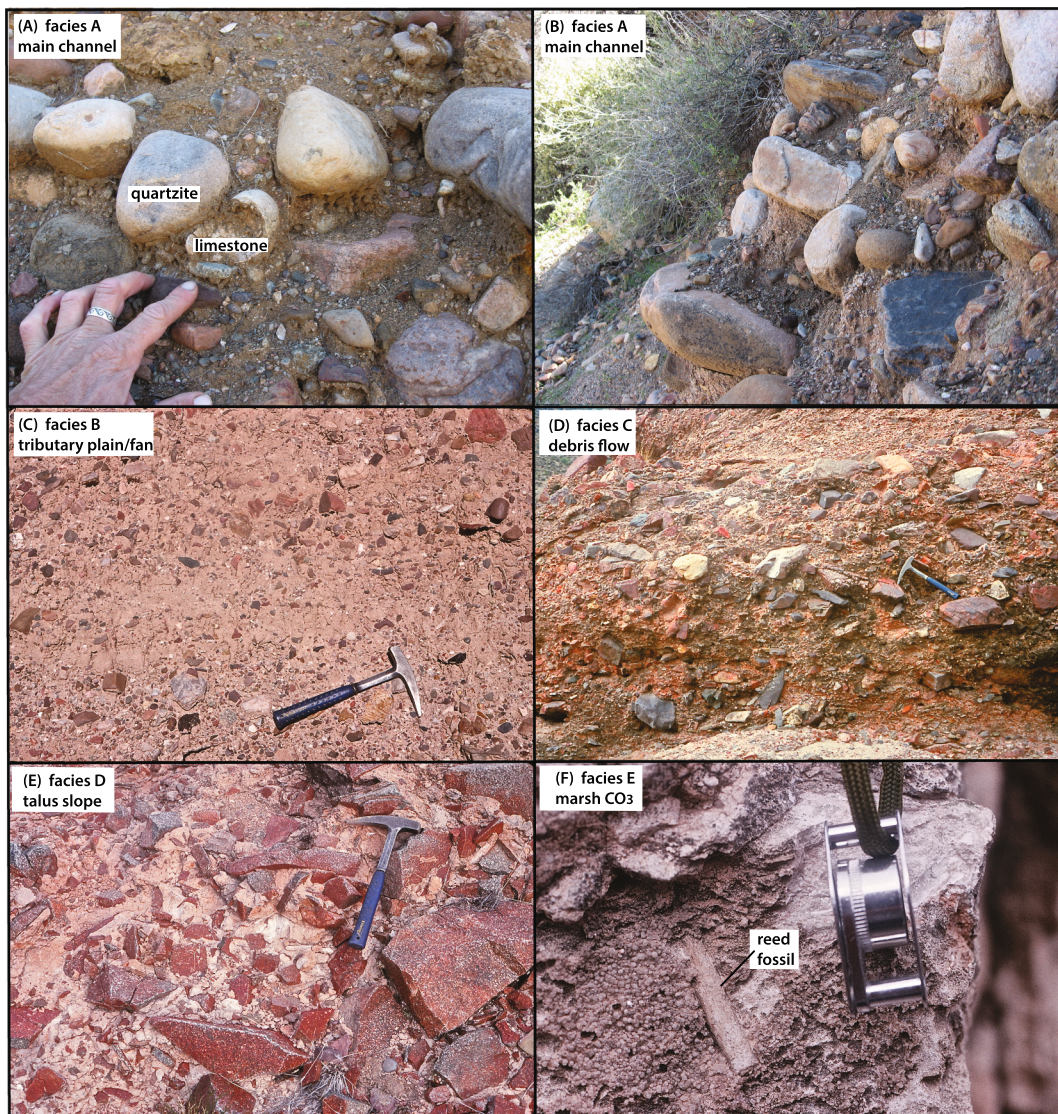


Fig. 6. Photos of facies A-E of Mogollon Rim sequence and Chalk Creek Formation west of Canyon Creek fault in Apache paleocanyon: (A) note stable quartzite and deep chemical weathering of limestone clast; (B) northeast imbrication of three quartzite boulders (~50 cm intermediate diameter) in basal conglomerate of Tm at mouth of Butte Creek; (C) locally derived, submature conglomeratic sandstone; (D) interbedded with angular matrix-supported debris flow conglomerate; (E) interbedded with monolithologic talus breccia on north flank of Apache paleocanyon wall; (F) dolomite with marsh fossil (*equisetum* sp.?) represents variety of ponded facies in Chalk Creek Formation.

stratigraphic position above pre-Cenozoic bedrock and below the Salt River sequence (Fig. 7). It is mostly free of Neogene mafic volcanic clasts but may contain siliceous volcanic and subvolcanic clasts of Laramide porphyritic rock, likely derived from the Globe-Miami mining district (Potochnik, 1989). The great variability of the Mogollon Rim sequence in thickness and lithology is governed by variations in paleotopography of the underlying erosion surface (Faulds, 1986; Potochnik, 2001a, 2001b; Richard and Spencer, 1998). West of Canyon Creek fault, the modern Salt River and its tributaries deeply incise the Mogollon Rim sequence but not deep enough to expose the Apache paleocanyon bedrock thalweg. Geologic mapping reveals the best exposed thalweg near the confluence of Butte Creek with the modern Salt River, directly west of Canyon Creek fault (Fig. 6). Here, the basal conglomerate of the Mogollon Rim Formation crops out in the walls of Butte Creek about 100 m from the Salt River channel (Fig. 6a, b) and is projected to overlie nearby outcrops of Proterozoic crystalline basement about 15–20 m below the Salt River. The Mogollon Rim Formation is gradationally overlain by the increasingly immature paleocanyon fill of the Whitetail facies (Fig. 7).

The Apache Ridge stratigraphic column is selected as the type section of the Mogollon Rim sequence west of Canyon Creek fault. It is central to a variety of intertonguing facies also observed in the adjacent reference section at Mud Springs Draw (Fig. 7). At Apache Ridge, the column rests on the southeast bedrock flank of Apache paleocanyon. The Mogollon Rim sequence is mostly fluvial in origin, with associated tributary plain, alluvial fan, debris flow, and colluvial facies (Potochnik, 2001a). Mature, facies A and B conglomeratic rocks comprise the basal 33 m of the Apache Ridge column and occupy the same stratigraphic position as the basal conglomerate of the Mogollon Rim Formation east of Canyon Creek fault (Potochnik, 1989). Similar facies A conglomerates are interbedded with Whitetail facies B, C, and D in most of these stratigraphic sections (Fig. 7). South of the Salt River near Bronson Canyon and Butte Creek, the Mogollon Rim sequence is a conformable stratigraphic unit intercalated near its base with the 37.60 Ma Bronson Canyon dacite flow and conformably overlain by the 18.63 Ma Apache Leap Tuff (Fig. 7, Table 1).

5.3.1.1. Paleocurrents and provenance. Paleocurrent measurements

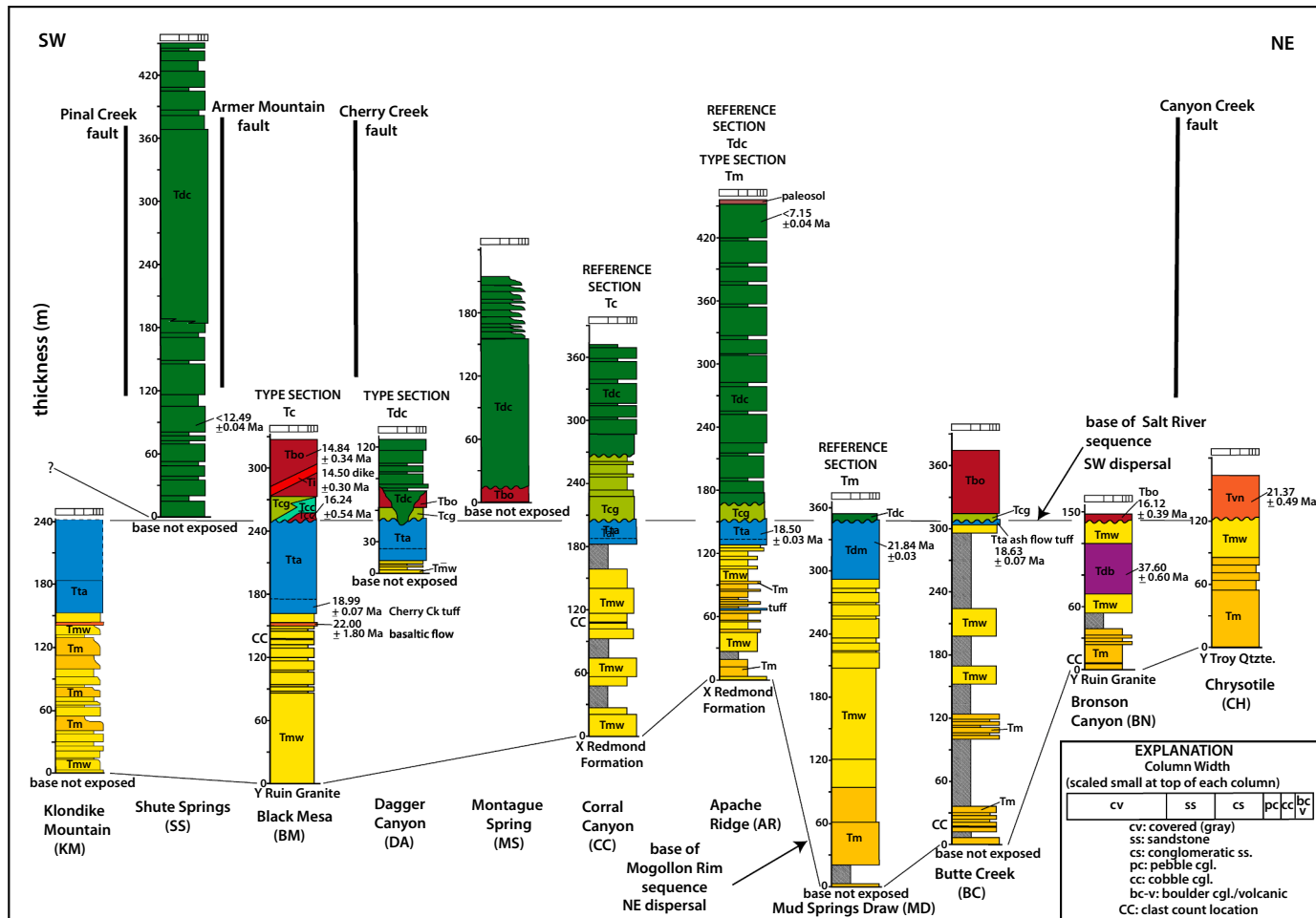


Fig. 7. Stratigraphic columns along axis of Apache paleocanyon. Columns are hung on the drainage reversal horizon at the unconformity above Apache Leap Tuff. Tie lines define base of Mogollon Rim and Salt River sequences.

from the Mogollon Rim sequence west of and slightly east of Canyon Creek fault are presented in Fig. 8. Within the main axis of Apache paleocanyon, the paleocurrent directions are dominantly toward the northeast, parallel to the paleocanyon topographic axis. Paleocurrent measurements for the Whitetail facies have an overall northeast-directed flow but have relatively high dispersion consistent with alluvial fans aggrading to and interfingering with facies along the main axis of the paleocanyon (Fig. 8). Based on the configuration of the underlying erosion surface, facies relations of the Mogollon Rim sequence and the thickness of infilling sedimentary units, Apache paleocanyon trends N50°E and extends from the Tonto Basin to Canyon Creek fault. The northeastward exit point of the axial stream from the Apache block closely corresponds with the path of the modern southwest-flowing Salt River (Fig. 8).

Along the north flank of Apache paleocanyon, paleocurrent directions are mostly to the southeast, whereas they are northerly or northeast south of the paleocanyon axis. These dispersal directions, along with facies relations and the configuration of the sediment–basement contact, define a main channel paleocanyon and two fault-controlled paleotributaries. From the north, *Cherry Creek paleotributary* trends south-southeast (Fig. 8), parallel to and coincident with Cherry Creek fault. Based on the paleocurrent data, it is inferred to have branched out toward the east once it exited the topographic confines along the fault zone. Near its confluence with the main channel Apache paleocanyon, sedimentary units associated with the paleocanyon become more widely distributed, and the associated sedimentary units have facies consistent with a broadening alluvial fan. The diverging

pattern of paleocurrent measurements would be expected in an alluvial fan setting (Bull, 1972).

The paleocurrent data indicate another paleotributary, *Butte Creek paleotributary*, coming from south of the main paleocanyon (Fig. 8). This paleotributary occupies an ancestral paleocanyon that trends northerly along the axis of Canyon Creek fault. It joins the main Apache paleocanyon directly east of the Apache uplift. Paleocurrents within the Butte Creek paleotributary define a northward mean vector direction parallel to Canyon Creek fault, but they show an unusually wide dispersion (Fig. 8). Provenance of the Mogollon Rim Formation in this region is determined by clast counts presented in the Regional provenance Section 5.6 below.

5.3.2. Apache Leap Tuff and associated volcanic rocks

The Apache Leap Tuff is a welded distal outflow sheet of ash-flow tuff (Faulds, 1989; McIntosh and Ferguson, 1998; Peterson, 1969). It overlies a weakly welded tuff here called the Cherry Creek tuff. Both tuffs (Tta) likely originated from the Superstition volcanic field east of Phoenix, 50 km southwest of the study area (Faulds, 1986; Ferguson and Trapp, 2001). These tuffs conformably overlie the Whitetail facies of the Mogollon Rim sequence within Apache paleocanyon (Fig. 9) and extend over a large region to the south and west (Fig. 1). Thickness of the Apache Leap Tuff outflow sheet is 600 m near the Superstition cauldron (McIntosh and Ferguson, 1998; Peterson, 1969), but the unit thins at its distal northeast margin from 116 to 3 m within the 27 km length of Apache paleocanyon (Faulds, 1986; Potocznik, 2001a). It is not known to crop out east of Canyon Creek fault.

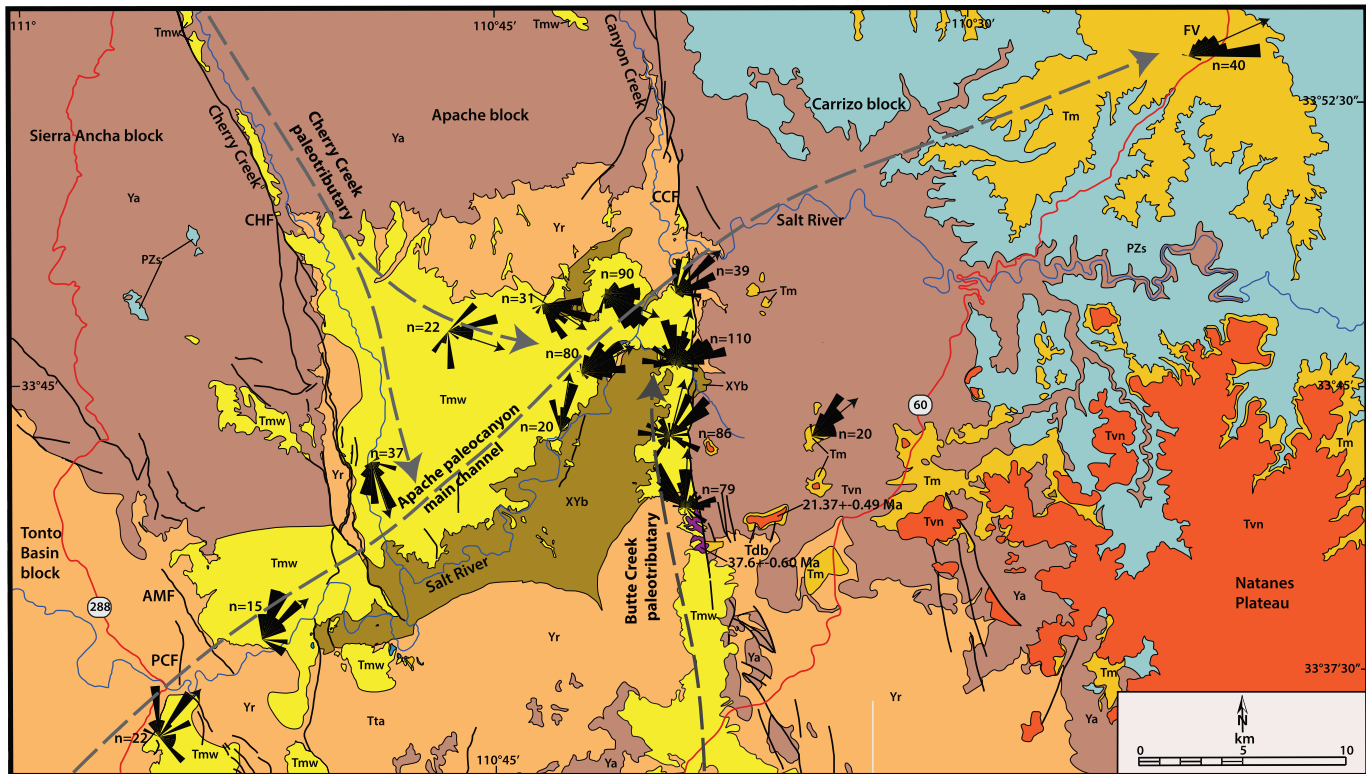


Fig. 8. Paleogeologic map of Fig. 3 showing sediment dispersal of Mogollon Rim sequence (Tm-Tmw) within Apache paleocanyon ca. 38–18.63 Ma.

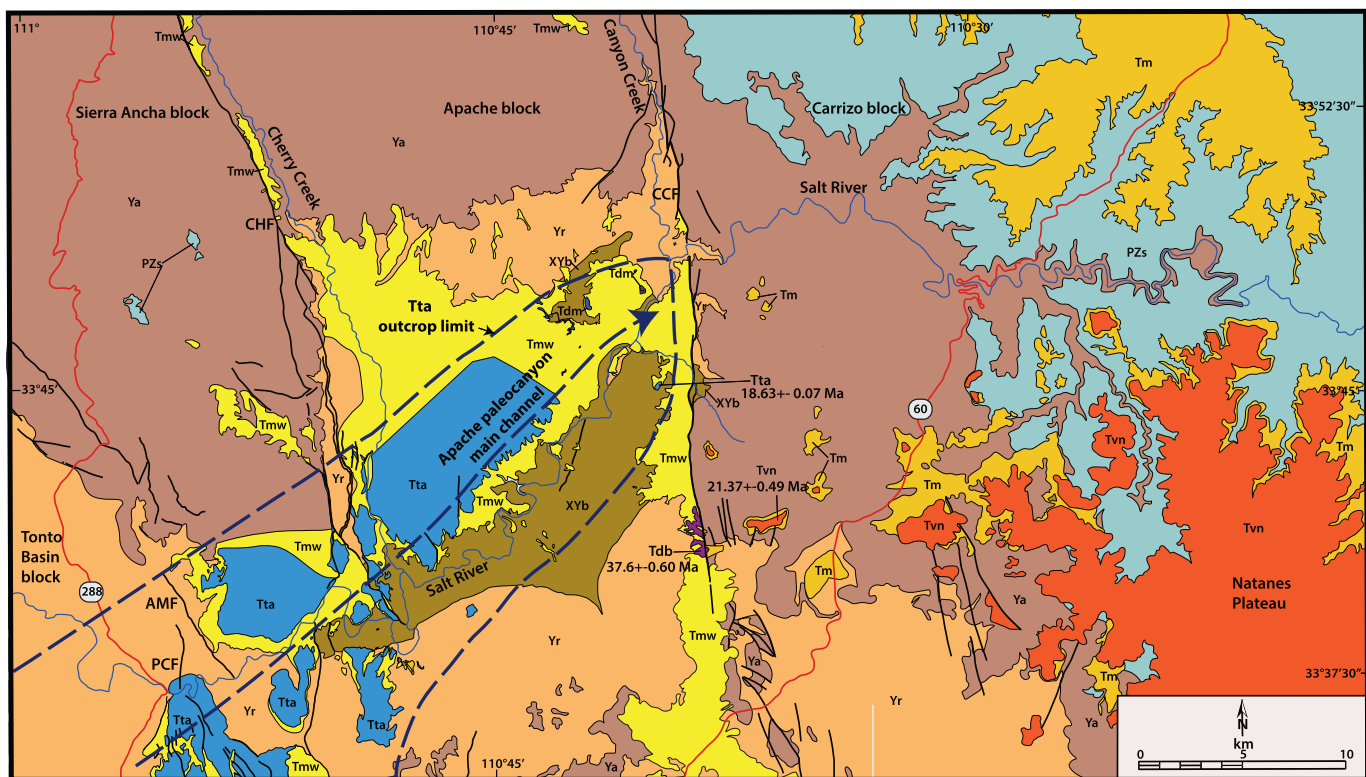


Fig. 9. Paleogeologic map of Fig. 3 showing Apache Leap Tuff (Tta) ash flow with northeastward dispersal within Apache paleocanyon at 18.63 Ma. Medicine Butte dacite (Tdm) shown in eastern Apache paleocanyon.

An $^{40}\text{Ar}/^{39}\text{Ar}$ age of 18.63 ± 0.07 obtained for the Apache Leap Tuff at its easternmost occurrence in the upper Butte Creek section just west of Canyon Creek fault (Fig. 7, Table 1) is statistically consistent with the mean age of 18.58 ± 0.03 Ma obtained for the tuff in its source region (McIntosh and Ferguson, 1998). These ages fall within similar ages obtained by other analyses in the area (Table 1) that suggest a broader period of eruptive history of the Superstition cauldron.

The Apache Leap Tuff exhibits regionwide depositional thinning to the northeast and becomes more weakly welded to the northeast along the length of Apache paleocanyon (Faulds, 1986; Potochnik and Faulds, 1998). Imbrication of gravels beneath the contact show continued northeast dispersal within the confines of Apache paleocanyon (Fig. 8), immediately prior to eruption of the tuffs. At this contact there is no evidence of scouring or soil development that would indicate a hiatus. It is reasonable to infer that a caldera-style eruption of regional magnitude would have outflow sheets that followed existing stream drainages northeastward and may have terminated against a developing Canyon Creek fault scarp (Fig. 9).

The Medicine Butte dacite flow (Tdm) caps Medicine and Canyon Creek Buttes (Figs. 4, 7) (Potochnik, 2001a). It crops out 1 km east of the Apache Leap Tuff pinchout at the same elevation and stratigraphic position, but its $^{40}\text{Ar}/^{39}\text{Ar}$ 21.8 Ma age (Canyon Creek dacite of Anderson et al., 2021) apparently predates the Apache Leap Tuff. An earlier attempt to date this flow by the same laboratory was considered indefinite and was not reported (Potochnik, 2001a). It is a felsic volcanic flow that issued from local vents in a relatively restricted outcrop area within the easternmost Apache paleocanyon (Fig. 9, Table 1).

5.4. Salt River sequence

Cenozoic sedimentary and volcanic units unconformably overlying or inset against the Mogollon Rim sequence are assigned to the Salt River sequence. The upper boundary of the Salt River sequence is the present day. It includes all Pliocene to Holocene terraces and volcanic flows that

occupy the modern Salt River canyon and its tributaries. As such, it is broad term that encompasses all geologic/geomorphic units formed after cessation of northeast-flowing streams and includes ponded and basin deposits. The type section for the Salt River sequence is Black Mesa, where the Chalk Creek Formation and intercalated basalts were first defined (Faulds, 1986). The reference section at Corral Canyon displays local variations in sedimentology and stratigraphy (Fig. 7).

5.4.1. Chalk Creek Formation and Black Mesa basalts

The Chalk Creek Formation (Tcg, Tcc) disconformably overlies the Apache Leap Tuff and occurs primarily within the confines of Apache paleocanyon. Submature alluvial and paludal layers (facies C–E) within the Chalk Creek Formation indicate sluggish stream transport, local ponding, and aggradation within and near Apache paleocanyon (Faulds, 1986; Potochnik and Faulds, 1998). The informally named Black Mesa basalt includes all basalt flows younger than the Apache Leap Tuff within Apache paleocanyon from Canyon Creek fault westward to the Tonto Basin. West of Cherry Creek, these flows conformably underlie and overlie the Chalk Creek Formation and have yielded K-Ar ages ranging from 16.24 ± 0.54 Ma to 14.84 ± 0.43 Ma (Damon et al., 1996; Faulds, 1986) (Figs. 7, 10). Black Mesa basalt flows occur at the Dagger Canyon, Montague Spring, Butte Creek, and Bronson Canyon sections. The Black Mesa basalt flows, intercalated in part with the Chalk Creek Formation, form the upper part of Apache paleocanyon fill sequence that accumulated prior to subsequent deep incision of these and underlying units by a southwest-flowing stream.

5.4.1.1. Paleocurrents and provenance. Paleocurrent data for the Chalk Creek Formation show high dispersion, with a tendency for southwest-directed flow directions (Fig. 10). We interpret these data to indicate that drainage integration was weakly developed for incipient southwest-flowing streams during this time. Notably, this southwest paleocurrent direction is opposite the underlying Mogollon Rim sequence (Figs. 8, 9).

Following deposition of the Black Mesa basalt in Apache

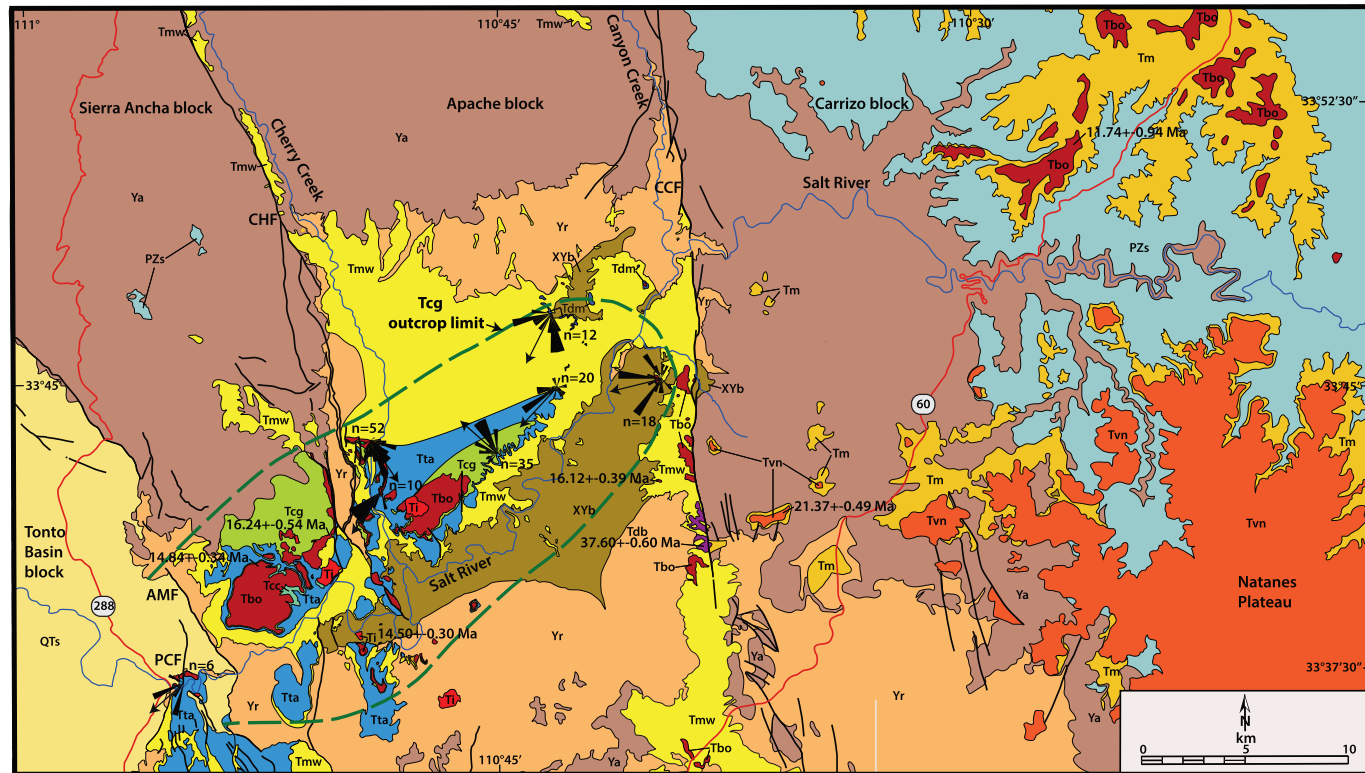


Fig. 10. Paleogeologic map of Fig. 3 showing sediment dispersal-ponding of Chalk Creek Formation (Tcg-Tcc) and interbedded-overlying Black Mesa basalts (Tbo) within Apache paleocanyon, $<18.63\text{--}14.84$ Ma.

paleocanyon, a 360-m-deep paleovalley is incised into the underlying Mogollon Rim sequence, Chalk Creek Formation, and Black Mesa basalts by a southwest-flowing stream parallel to and nearly coincident with Apache paleocanyon, the Dagger Canyon paleovalley. The southwestward flow direction is evidenced by the shape of the erosion surface and its paleovalley fill deposits (Figs. 3, 5). This incision of canyon-fill deposits is the earliest unequivocal record of regional drainage reversal across the Transition Zone. It occurred after the 14.50 ± 0.30 Ma intrusion of the Shendaby dacite plug (Faulds, 1986) (Table 1; BM in Fig. 7). Following this incision event, a carbonate soil developed on the flanks of Dagger Canyon paleovalley prior to deposition of Dagger Canyon Conglomerate within the paleovalley.

5.4.2. Dagger Canyon Conglomerate

The Dagger Canyon Conglomerate (Tdc) comprises well-sorted facies A conglomeratic arkose. The conglomerate is named for a tributary to Cherry Creek that reveals its thalweg and is near several key exposures. It is restricted to areas within the Dagger Canyon paleovalley (Figs. 5, 11) and overlies in buttress unconformity all previous Cenozoic paleocanyon deposits (Fig. 3 in Potochnik, 2001b; graphical abstract, this paper). It is primarily composed of gravel and sand reworked from outcrops of the Mogollon Rim Formation east of Canyon Creek fault (Potochnik and Faulds, 1998), marking a sharp contrast with the underlying poorly sorted gravels of the Whitetail facies and Chalk Creek Formation. Deposition of the Dagger Canyon Conglomerate within the Dagger Canyon paleovalley reached nearly the same elevation as the earlier deposited Whitetail facies and Chalk Creek Formation (Fig. 5). It thickens westward from Canyon Creek fault to the Tonto Basin where it is downfaulted and overlain by more recent Tonto Basin sediments (Fig. 3) (Nations, 1988). The Dagger Canyon Conglomerate terminal depocenter may be the Tonto Basin (Anderson et al., 2021) or it may have extended southwestward to the Higley Basin where preserved as Rolls formation on the west flank of the Mazatzal Mountains (Skotnicki et al., 2020).

Between Tonto and Higley basins, Rolls formation is distributed over a large region along the north flank of the modern Salt River (Skotnicki et al., 2020). Lithologic data from well cuttings suggests that Rolls formation descends southwestward stratigraphically beneath ancestral Salt River deposits (ASRD) into the Higley basin (Dorn et al., 2020; Larson et al., 2020; Skotnicki and DePonty, 2020). The Rolls formation may be contiguous with the Stewart Mountain fluvial terrace, the uppermost of sequentially lower terraces that characterize Quaternary development of the modern Salt River (Larson et al., 2010). Further work is needed to determine lithostratigraphic and geomorphic relations of the Rolls formation to the subsurface Higley Basin deposits (e.g. Larson et al., 2020; Reynolds and Bartlett, 2002).

Preliminary observations by the first author of Rolls formation along Cottonwood Creek suggest lithostratigraphic correlation with Dagger Canyon Conglomerate in Apache paleocanyon. Abundant rounded white quartzites (Proterozoic Troy, White Ledges Quartzites), 40 cm well-rounded granite boulders, deeply in situ weathered porphyritic latite clasts (Mount Baldy volcanics?), and felsic ash flow gravels (Apache Leap Tuff?) are deposited in an arkosic sand matrix with partial clast support of gravels (facies A). Imbrication of gravels indicates northwesterly deposition, orthogonal to the southward surface erosion rills ("The Rolls") directed toward the modern Salt River. Along Cottonwood Creek the Rolls formation is juxtaposed against a 100 m thick welded ash flow tuff that overlies Whitetail facies gravels tilted gently to the southwest. This set of geomorphic and sedimentologic observations is similar to that observed at the Dagger Canyon Conglomerate type locality in Apache paleocanyon.

The Dagger Canyon Conglomerate and its various facies (Potochnik, 2001a) are briefly described at four key localities (Fig. 7). The type section at Dagger Canyon (DA) is clast-supported mature fluvial conglomerate deposited in the thalweg of Dagger Canyon paleovalley. The reference section in the Apache Ridge (AR) column reveals a thicker section and includes its capping mollisol paleosol formed before incision of the modern Salt River (Fig. 5). Nearby sections at Montague Spring,

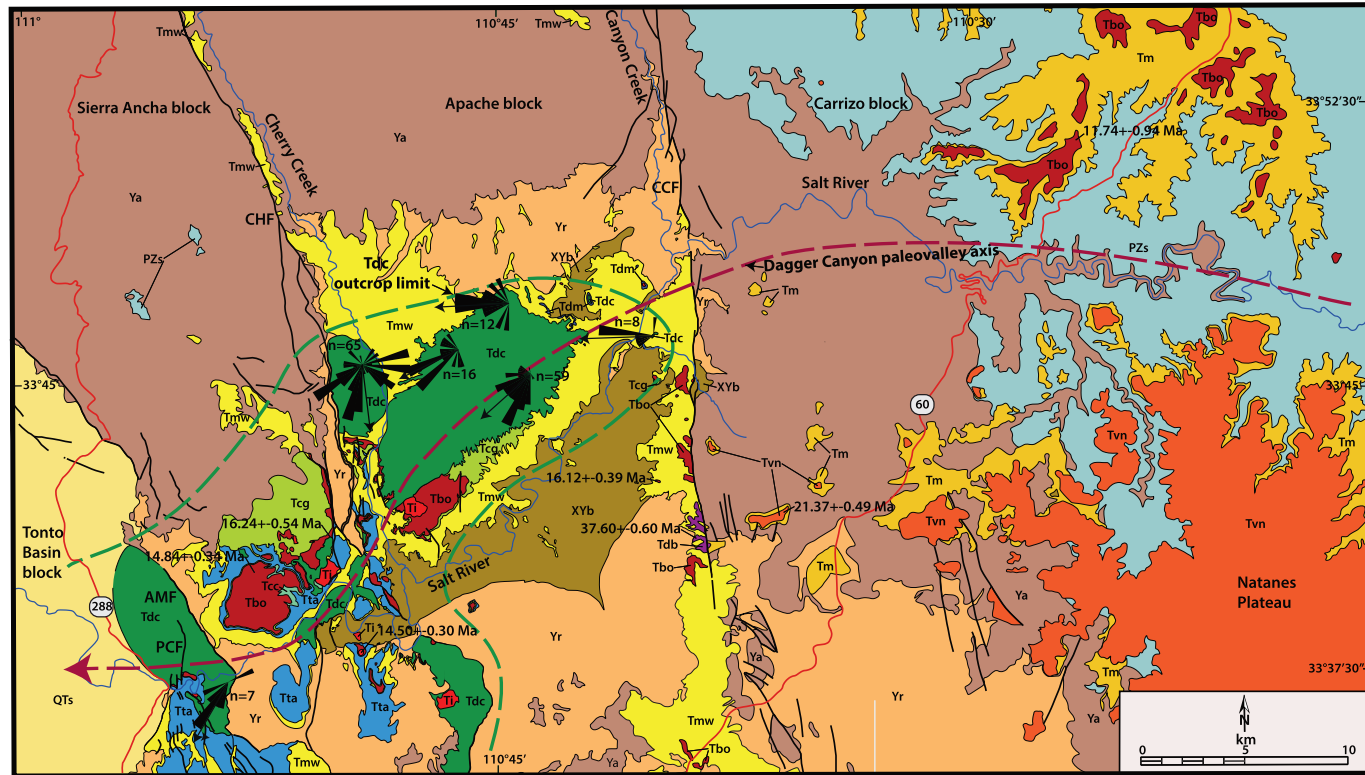


Fig. 11. Paleogeologic map of Fig. 3 showing sediment dispersal of Dagger Canyon Conglomerate (Tdc) inset within Dagger Canyon paleovalley, ca. 14.84 to <7.1 Ma.

Coon Creek, and Shute Springs illustrate the variety of interfingering facies within Dagger Canyon Conglomerate (Fig. 7).

5.4.2.1. Paleocurrents and provenance. The Dagger Canyon Conglomerate exhibits southwest dispersal patterns (Fig. 11), similar to those for the underlying Chalk Creek Formation. However, the mean vectors are more consistent and the overall data dispersion is minimal, reflecting a through-going and integrated drainage system. The provenance of the Dagger Canyon Conglomerate is primarily arkosic sands and mature conglomerate reworked from the Mogollon Rim Formation with a minor component of olivine basalt and distinctive Mount Baldy latite porphyry clasts.

5.5. Cenozoic stratigraphy east of Canyon Creek fault and north of Apache paleocanyon

North of Apache paleocanyon and east of Canyon Creek fault the Cenozoic section overlies an erosion surface variously incised into or beveled across progressively younger strata to the north and east. This erosion surface comprises strata ranging in age from the Mesoproterozoic Apache Group to late Cretaceous marine shoreline sandstone (Fig. 1). The Cenozoic rocks underwent southward flexure of the Transition Zone, causing them to lie at progressively lower elevations today (Potochnik, 1989). Earlier work in this region east of Canyon Creek fault is reviewed here and is augmented with subsequent work north of Apache paleocanyon (Fig. 12). The Cenozoic strata are described below from oldest to youngest.

5.5.1. Round Top Mountain formation

We propose the name Round Top Mountain formation (Tr in Fig. 2) for this distinctive redbed unit of probable Paleogene age (Potochnik, 1989) with the name taken from the corresponding nearby topographic feature (Round Top Mtn., Ariz. 7.5" USGS quadrangle). The type section crops out on a southward spur of the Mogollon Rim at Round Top Mtn south of the town of Show Low, AZ (RT in Fig. 1, UTM 3755.0N, 590.72E, 0.92 km west of the top of Round Top Mountain at 6600 ft elevation). Here, Cenomanian marine sandstone of the Dakota Group (Cobban and Hook, 1984; Molenaar, 1983) unconformably overlies Permian Coconino Sandstone (K1 in Fig. 2). The Dakota Group sandstone is, in turn, unconformably overlain by the Round Top Mountain formation (T1 in Fig. 2) which is, in turn, unconformably overlain by the Mogollon Rim Formation (T2 in Fig. 2). Round Top Mountain is topographically held up by a 28 Ma rhyolite volcanic neck that intrudes this stratigraphic sequence (Peirce et al., 1979; Potochnik, 1989). The outcrop area is too small to show on Fig. 1.

The Round Top Mountain type section comprises a 1–2 m thick basal cobble/pebble conglomerate overlain by 30 m of mudstone redbeds that contain a 3 m thick, purple fluvial pebbly sandstone. This relatively fine-grained fluvial formation is unconformably and sharply overlain on an irregular erosion surface by light-colored, basal boulder conglomerate of the Mogollon Rim Formation (Potochnik, 1989). This formation, if present west of Canyon Creek fault, is not preserved/observable due to burial of Apache paleocanyon thalweg. There is a lithologically and stratigraphically similar unit of fluvial redbeds described in the Alpine1/Federal corehole 62 km east of this study location (Witcher et al., 1994).

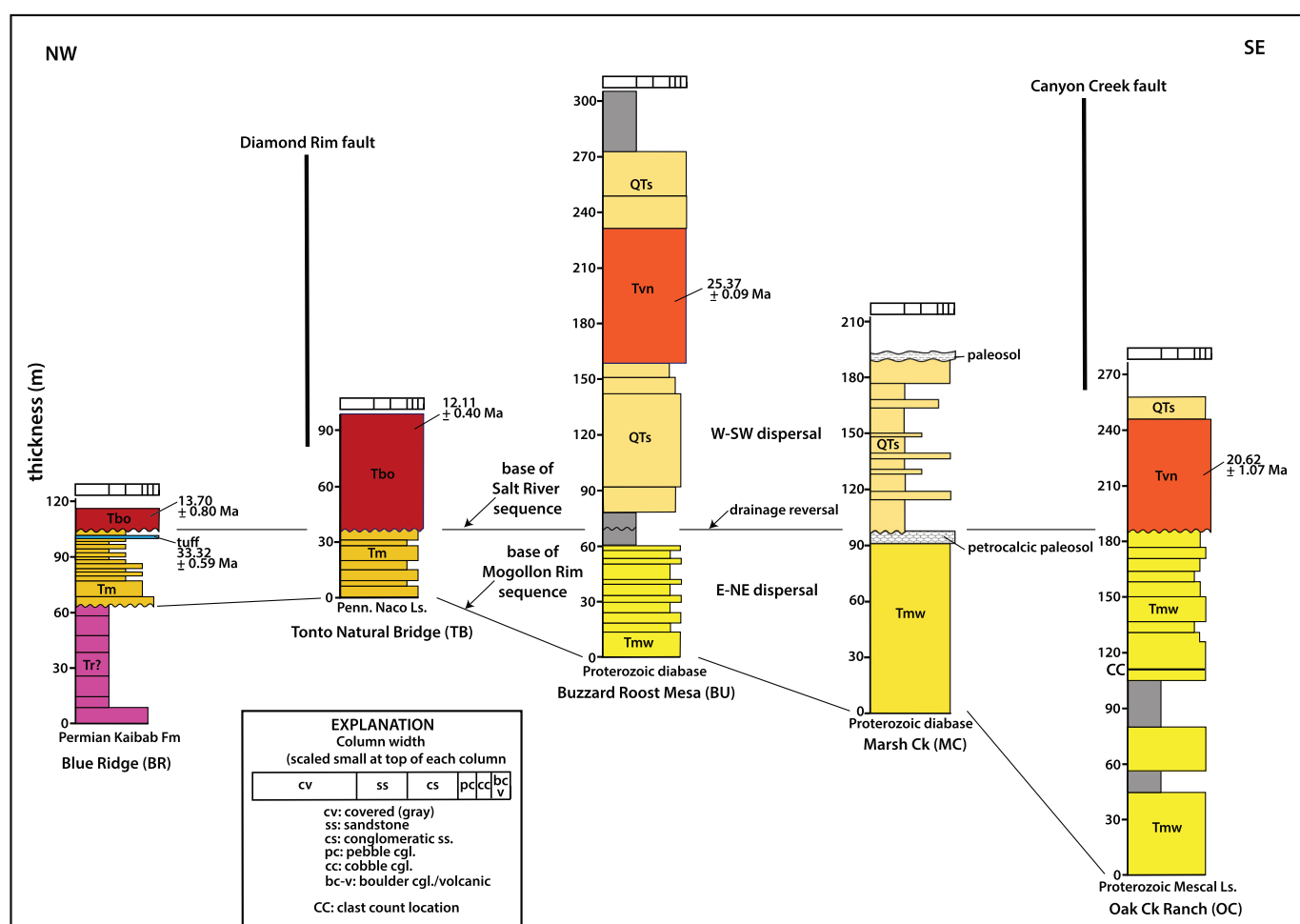


Fig. 12. Stratigraphic columns west of Canyon Creek fault and north of Apache paleocanyon to the Mogollon Rim region (Fig. 1). Columns are hung on the drainage reversal horizon. Tie lines define base of Mogollon Rim and Salt River sequences.

The Round Top and Alpine1/Federal early Cenozoic redbed sections are lithostratigraphically similar to the Middle to Late Eocene Baca Formation of western New Mexico and easternmost Arizona (Cather et al., 1994). The Round Top Mountain formation occupies a hiatus spanning the period from Cenomanian to Late Eocene (ca 94–40 Ma).

A similar fluvial redbed sequence 61 m thick unconformably overlies the Permian Kaibab Formation at the Blue Ridge section (BR in Fig. 12) at the most northwesterly exposure of the Mogollon Rim Formation (Fig. 1). Presently mapped as Triassic Moenkopi Formation (Richard et al., 2000), these redbeds overlie a 10 m thick basal limestone clast conglomerate and are unconformably and sharply overlain by light-colored basal boulder conglomerate of the Mogollon Rim Formation (Figs. 2, 12). Additional work is needed to resolve whether the age of the Blue Ridge redbed outcrop is Triassic or Paleogene.

5.5.1.1. Paleocurrents and provenance. At the type section (RT in Fig. 1), clast imbrication and dip azimuth of planar crossbeds ($n = 4$) provide a mean vector of N76 E. The presence of porphyritic intermediate volcanic (35%), granite (5%), quartzite (10%), and Paleozoic-Cretaceous clasts (50%) indicate a southwesterly provenance for the Round Top Mountain formation. Geographic setting, stratigraphic position, and northeastward dispersal direction of conglomerates suggest correlation of the Round Top Mountain formation with the “unnamed Cretaceous-Tertiary?” strata in the Alpine1/Federal corehole (Witcher et al., 1994).

5.5.2. Mogollon Rim Formation

North of Apache paleocanyon and east of Canyon Creek fault a series of stratigraphic columns delineate a similar paleogeography (Fig. 12). Facies A and B conglomeratic sequences that overlie the Round Top Mountain formation (?) at Blue Ridge (BR) and overlie Pennsylvanian Naco Formation at Tonto Natural Bridge (TB) (Fig. 1) are correlated with the Mogollon Rim Formation based on geographic location proximal to the Colorado Plateau and the age of an interbedded tuff near the top of the Blue Ridge section dated at 33.32 ± 0.59 Ma (Fig. 12, Table 1). At Tonto Natural Bridge, Permian rocks were eroded away prior to deposition of the sediments but are still preserved on the Mogollon Rim to the north. Sections of Cenozoic conglomerate at both Tonto Natural Bridge and Blue Ridge are unconformably overlain by Middle Miocene basalts (Fig. 12, Table 1), defining a hiatus that represents most of Oligocene and Early Miocene time.

The facies A conglomeratic sequences that overlie Paleozoic and Upper Cretaceous strata at the Young Road and Chediski Ridge localities (Fig. 1) are also correlated with the Mogollon Rim Formation based on geographic location, stratigraphic position, and overall composition. The Young Road outcrops (YR in Fig. 1) define the north wall of *Chediski paleocanyon*, here defined, where they are deposited in buttress unconformity against a south-facing ancestral escarpment incised into Proterozoic through upper Paleozoic rocks. This ancestral escarpment exhibits as much as 700 m in paleotopographic relief parallel to the modern Mogollon Rim (Skotnicki, 2002, B-B' cross section), as first described by Peirce et al. (1979). The Mogollon Rim Formation near Tonto Natural Bridge is in a similar paleotopographic setting, so may also represent part of Chediski paleocanyon. Chediski paleocanyon is not evident east of Canyon Creek fault along Chediski Ridge (CR in Fig. 1) and onto the Colorado Plateau.

Other exposures north of Apache paleocanyon (Buzzard Roost Mesa, Marsh Creek, Bottle Spring, Keystone Ridge, and Oak Creek Ranch) are characterized by facies B and C fanglomerates clearly ancestral to and unrelated to modern stream systems. They are consolidated, perched on ridges or swales above modern canyons, and generally widely distributed in the local area (Fig. 1). The lower part of Cenozoic sections at Buzzard Roost Mesa, Marsh Creek, and Oak Creek Ranch are assigned to the Whitetail facies of the Mogollon Rim sequence (Tmw). The upper parts of these three sections are assigned to the Salt River sequence (QTs) based on their dispersal directions (Fig. 12). Proximal alluvial fan

facies characterize all three columns both below and above the drainage reversal unconformity (see Sections 5.7, 5.8).

East of Canyon Creek fault, the Mogollon Rim Formation is a broadly distributed alluvial braidplain sequence of far-traveled mature gravels and arkosic sandstone (Potocznik, 1989). The formation thins to the west-southwest from 375 m at the Trout Creek (TC) type section (Potocznik, 1989) to 120 m at Chrysotile (CH in Fig. 7), and 45 m at Blue Ridge (BR in Fig. 12). ^{40}Ar - ^{39}Ar ages of 35.22 and 33.55 Ma (Table 1) provide a depositional rate for the upper Mogollon Rim Formation that extrapolates down section to ca. 36.8 Ma for the onset of deposition at the Trout Creek type section east of Canyon Creek fault (Fig. 2). This extrapolated age is comparable to the 37.60 Ma rhyodacite flow intercalated in the basal Mogollon Rim sequence at Bronson Canyon (BN) west of Canyon Creek fault (Fig. 7, Table 1).

The Mogollon Rim Formation was previously correlated with the Middle to Late Eocene Baca Formation of west-central New Mexico (Cather and Johnson, 1984; Potocznik, 1989; Potocznik and Faulds, 1998). Lithostratigraphically the Mogollon Rim Formation more aptly correlates with the Eagar Formation (Surrine, 1958) of eastern Arizona and as observed in the well core of Alpine1/Federal geothermal corehole at the Alpine divide east of Mount Baldy (Witcher et al., 1994). It is possible that the Roundtop Mountain formation and Mogollon Rim Formation merge laterally with the Baca Formation in western New Mexico (Cather et al., 1994).

5.5.3. Spears Group and overlying volcaniclastic rocks

The Mogollon Rim Formation near its type section on the Mogollon Rim (TC) is variably overlain both gradationally and unconformably by volcaniclastic strata that range in thickness due to complex stratigraphic relationships near the Mogollon Rim. Unconformities between these volcanic/volcaniclastic formations are shown in Fig. 2 (T3a, T3b, T3c). The primary fluvial volcaniclastic unit is the Spears Group (Tvs1) as described in the Quemado-Escondido Mountain area of western New Mexico, where the unit conformably overlies the Middle to Late Eocene Baca Formation and attains a thickness of 781 m (Chamberlin and Harris, 1994). In this area, the Spears Group is overlain by the widespread Bearwall Andesite dated at 26.1 Ma (McIntosh and Chamberlain, 1994). This stratigraphic sequence is preserved beneath the Mount Baldy shield volcano complex as described in the Alpine1/Federal corehole near Alpine, AZ (Witcher et al., 1994), located about 62 km east of the Trout Creek type section of the Mogollon Rim Formation. Here, the corehole reveals 625 m of Spears Group with as much as 352 m of additional Oligocene section, most of it equivalent to eolian Chuska Sandstone, exposed along the flank of Escudilla Mountain north of the corehole (Cather et al., 2008). The overlying and inset fluvial volcaniclastics (Tvs2, Tvs3) are described below in cross sections at or near the modern Mogollon Rim (Section 5.10).

At Nash Canyon (NC in Fig. 1) 200 m of fluvial volcaniclastic conglomerates, temporally equivalent to the Spears Group (Tvs1), fill a channel incised in the upper Mogollon Rim Formation. These conglomerates are unconformably overlain by the Middle Miocene Natanes Plateau basalt flows (Potocznik, 1989) (Fig. 2). An intercalated ash-fall tuff with an age of 34.15 ± 0.60 Ma (Table 1) provides a constraint for the onset of volcaniclastic sedimentation in this region (Section 5.10).

At Deep Creek (DC in Fig. 1), the upper Mogollon Rim Formation, dated at 35.21 ± 0.40 Ma (Table 1), is gradationally overlain by tuffaceous sandstones of the Spears Group (Tvs1) that increasingly overwhelm the arkosic basement-derived sands from the ancestral Mogollon highland to the southwest. Lahars and autobrecciated intermediate volcanic rocks are intercalated in the section, which thickens eastward beneath the Late Miocene Mount Baldy volcanic field to over 536 m (Tvv of Merrill and Pewe, 1977) at the uppermost reaches of the East Fork of White River (EF in Fig. 1).

At Trout Creek (TC in Fig. 1), the uppermost Mogollon Rim Formation (33.55 ± 0.41 Ma) is gradationally overlain by a 30-m-thick remnant of tuffaceous sandstone of the Spears Group (Tvs1). Here, the

Spears Group thickens eastward beneath the Mount Baldy volcanic complex to at least 664 m at Tiger Butte (TB in Fig. 1) (Tvv of Merrill and Pewe, 1977). At Trout Creek, the Spears Group is deeply eroded and overlain in buttress unconformity by fluvial volcaniclastic conglomerates (Tvs2) with an intercalated basaltic andesite flow dated at 24.8 Ma (Damon et al., 1996; Potochnik, 1989).

At Juniper Ridge (JR in Fig. 1) on the Colorado Plateau southern margin, a thin veneer of residual volcaniclastic sandstone (Tvs3) unconformably overlies the erosionally-deflated Mogollon Rim Formation “rim gravel”. This outcrop contains detrital zircon populations that span from Proterozoic through Miocene ages, the youngest spike dated at 18.6 ± 2.7 Ma (Potochnik et al., 2012).

5.5.4. Natanes Plateau basalts

The Natanes Plateau is a large region of laterally extensive basalt flows that occupy the Transition Zone south of the Colorado Plateau margin (Fig. 1) (Reynolds et al., 1986). One significant eruptive center is located at Grindstone Mountain (GM) about halfway between Nash Canyon (NC) and Deep Creek (DC) (Fig. 1). There, 13 olivine basalt flows diminish to the southwest to just 2 flows. This volcanic plateau lies at about the same elevation as the southern Colorado Plateau to the north and is physiographically contiguous with that region. It is deeply incised by the White River, the primary northern tributary of the Salt River, forming a large arcuate erosional embayment in the two plateaus (“Carrizo embayment” of Reynolds et al., 1986; Damon et al., 1996; Potochnik, 1989). The Natanes Plateau volcanic flows unconformably overlie the Mogollon Rim Formation and Spears Group fluvial volcaniclastic rocks over much of the region east of Canyon Creek fault, providing constraints on the hiatus following deposition of the Mogollon Rim Formation. K-Ar ages for the Natanes Plateau and its accordant erosional outliers in the Salt River drainage range from 24.76 ± 0.48 Ma at Trout Creek to 20.62 ± 1.07 Ma at Oak Creek Ranch (Damon et al., 1996) (Fig. 1). The absence of these widespread flows on the Colorado Plateau suggests topographic blockage of these basalts northward of the Transition Zone province.

5.5.5. Bidahochi Formation

The Bidahochi Formation was deposited in the modern Little Colorado basin on the southern Colorado Plateau immediately north of Fig. 1 (Dallege et al., 2003). The Bidahochi primarily overlies a broad and gently-dipping, northeast-beveled erosion surface of Triassic to Cretaceous strata. It is described as comprising six members; 1–4 primarily lacustrine; 5 primarily volcanic; and, 6 primarily fluvial. Interbedded volcanic ashes and volcanic flows provide ages that range from 15.5 to 6.62 Ma. Aggradation rates for the lower members 1–2 are 25–35 m/m.y. which drop to 7 m/m.y. for members 3–4 between 13.7 and 7.7 Ma. Granule conglomerates in member 4 are the only gravel facies described in the Bidahochi with the exception of a local thin basal conglomerate (Douglass et al., 2020). The Bidahochi Fm is presented here as to its possible paleogeographic connection to the Dagger Canyon paleovalley.

5.5.5.1. Paleocurrents and provenance. Douglass et al. (2020) provide a thorough discussion on this topic that is not repeated here. An ancestral Colorado River carrying a similar sediment load to the modern river does not account for the relative small volume of sediment in the Bidahochi Formation over the roughly 10 m.y. timespan of its existence, suggesting the possibility that it was never a closed basin (Dallege et al., 2003). The upper fluvial-dominated member may have prograded westward toward an eventual fluvial exit through modern Grand Canyon (Douglass et al., 2020). An exit for the lower lacustrine-dominated members may have been through an ancestral eastern Grand Canyon (Karlstrom et al., 2017) and/or through the Dagger Canyon paleovalley (Potochnik, 2011).

5.5.6. Mount Baldy volcanic field

The Mount Baldy volcanic field is a latite and basalt shield volcano complex emplaced on the eastern terminus of the Mogollon Rim in Arizona between about 9.83 ± 0.21 Ma (Damon et al., 1996) and 8.66 ± 0.19 Ma (Condit and Shafiqullah, 1985). The tops of the two shield volcanoes reach elevations of nearly 3475 m (11,400 ft), well above the elevation of the Mogollon Rim and Natanes Plateau, which generally range from 1950 to 1980 m (6400 to 6500 ft). The Mount Baldy volcanic field overlies the Natanes Plateau, Spears Group, and Mogollon Rim Formation in the northeast part of the study area (Fig. 1). This basalt-latite shield volcano complex was emplaced on a southwest paleoslope (Merrill and Pewe, 1977).

5.5.7. Springerville volcanic field

The Springerville volcanic field is composed of Pliocene-Pleistocene basalt flows that erupted from and were emplaced over a broad region on the southern periphery of the Colorado Plateau in eastern Arizona (Fig. 1) (Condit et al., 1994; Crumpler et al., 1994). Several flows continued southward off the Mogollon Rim and were emplaced for tens of kilometers along the bottom of modern tributaries of the Salt River. Today, they remain as erosional remnants perched tens of meters above the modern White River, Salt River, and their tributaries. These flows along the modern canyon bottoms range in age from 3.0 to 0.60 Ma (Anderson et al., 2021; Condit and Connor, 1996; Condit and Shafiqullah, 1985; Condit et al., 1994; Damon et al., 1996; Peirce et al., 1979).

5.6. Regional provenance of Mogollon Rim Formation

Clast counts in conglomerates document variation in provenance of the Mogollon Rim Formation depositional system. Counts were conducted in an east-northeast-oriented transect along the axis of Apache paleocanyon and northward along strike of Canyon Creek fault from Apache paleocanyon to the Mogollon Rim (Fig. 13). The purpose of the former is to assess provenance parallel to depositional slope along the axis of Apache paleocanyon. The purpose of the latter is to assess provenance parallel to the ancestral mountain front of the Apache uplift. Fig. 13 includes an additional six clast count sites northeastward from Canyon Creek fault across the Mogollon Rim Formation ancestral alluvial plain (from Potochnik, 1989).

Clast types in the Mogollon Rim Formation are grouped into five categories that reflect the primary rock units of the pre-Cenozoic geology.

1. Metamorphic rocks: The Alder-Red Rock Groups (ca. 1.7 Ga; Conway and Silver, 1989) and Mazatzal-Hess Canyon Groups (ca. 1.5–1.7 Ga; Cuffney, 1976; Doe et al., 2012; Livingston, 1969) are regionally extensive outcrops of the metasedimentary and metavolcanic basement in the Transition Zone and are combined on the maps of this report (XYb, Fig. 1).
2. Granitoids: The Proterozoic granitoids comprise the locally extensive Ruin Granite (ca. 1.4 Ga; Berquist et al., 1981) and Proterozoic “red” granites (ca. 1.7 Ga; Anderson, 1989). Laramide granitoids from the Globe-Miami mining district (southwest of this area) may also contribute to this category (Ransome, 1903) (XYb in Fig. 1, Yr in Fig. 3).
3. Apache Group, Troy Quartzite, and associated diabase (ca. 1.2–1.0 Ga; Schrire, 1967): Late Proterozoic epiclastic sedimentary rocks and diabase sills comprise most of the pre-Cenozoic landscape in this part of the Transition Zone. The clasts are dominantly Dripping Spring Quartzite and diabase with lesser contributions from the Pioneer Shale, Mescal Limestone and Troy Quartzite (Ya in Fig. 1).
4. Paleozoic sedimentary rocks: Include limestone, chert, sandstone, and shale (Berquist et al., 1981; Cuffney, 1976; Moore and Peirce, 1967) (PZs in Fig. 1).

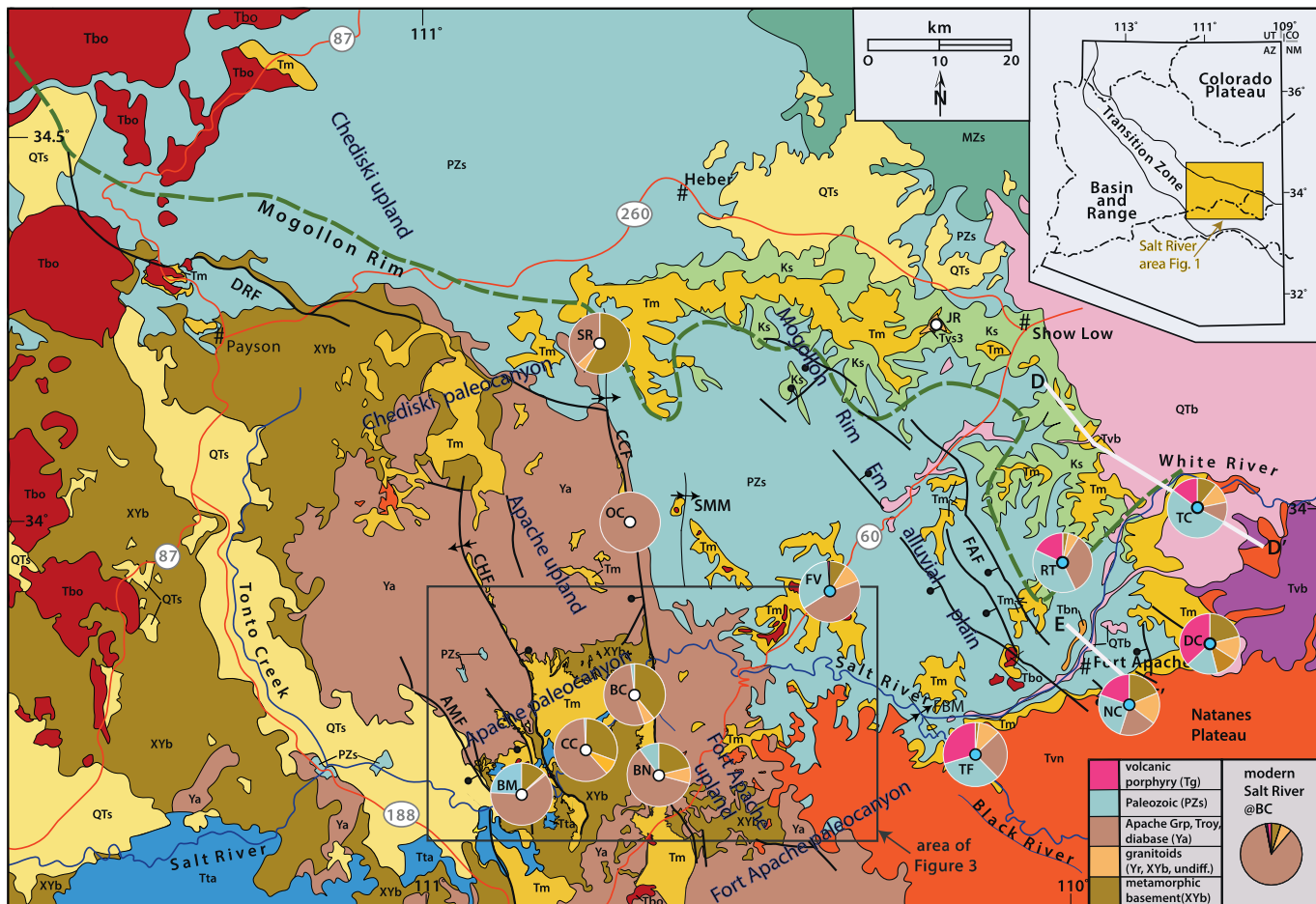


Fig. 13. Provenance of Mogollon Rim sequence outcrops (Tm-Tmw) from gravel clast counts: west of Canyon Creek fault, this study; east of Canyon Creek fault after Potochnik (1989). Lithologic associations color-coded to Fig. 2 with QTs sedimentary cover partly removed for clarity. Typically, 100–250 clasts counted per site larger than 2 cm within 1 m diameter outcrop exposure, site randomly selected. Inset shows modern Salt River clast count for comparison measured at Butte Creek (BC) mouth. Ancestral paleogeographic features (blue lettering) are interpretations based on dispersal (Fig. 14), provenance, paleotopographic, and geochronologic data. (For interpretation of the references to color in this figure legend, the reader is referred to the web version of this article.)

5. Volcanic porphyries: Intermediate-composition igneous rocks with bimodal grain size and lacking metamorphic foliation. Phenocrysts are mostly plagioclase and hornblende, with lesser pyroxene, quartz, and biotite. Groundmass colors vary and are typically gray, green, or red. This distinctive suite of Laramide rocks includes shallow level intrusions likely eroded from above the coeval granitoids in the Globe-Miami mining district southwest of this area (Peterson, 1969; Potochnik, 1989; Ransome, 1903).

Four clast-count localities parallel the northeastward depositional slope of Apache paleocanyon axis, from Black Mesa (BM) in the southwestern part of Apache Canyon paleocanyon, through intermediate sites Corral Canyon (CC) and Butte Creek (BC), and toward a distal alluvial-plain correlative (Potochnik, 1989) at Flying V (FV) (Fig. 13). At the first three localities within Apache paleocanyon, Alder Group and Red Rock Group basement clasts are absent, and granitoids are a minor but consistent component. The Mazatzal Group and Hess Canyon Group clasts systematically increase in abundance from 13% to 41% toward the northeast, reflecting ancestral upstream influx from the Mazatzal Mountains region and local influx from extensive exposures of the Hess Canyon Group within Apache paleocanyon. They decrease to 9% at the more ancestral downstream Flying V alluvial plain outcrop. Paleozoic limestones decrease in abundance along the axis of the paleocanyon from 24% at Black Mesa northeastward to 2% at Butte Creek then increase to 33% at Flying V. The abundance of Paleozoic limestones at

Black Mesa indicates provenance from the region southwest of the Apache uplift, where Paleozoic rocks are relatively abundant (Richard et al., 2000). In the central part of Apache paleocanyon, Paleozoic clasts are nearly absent, suggesting that they had been mostly stripped from the surface of the adjacent plateaus prior to onset of fluvial deposition. The increase in Paleozoic clasts to the northeast at Flying V and other locations in that region reflect the predominance of underlying Paleozoic limestones in the substrate. These trends demonstrate that provenance of the Mogollon Rim sequence in Apache paleocanyon was strongly dominated by locally derived rocks and that the axial trend of the main paleocanyon extended southwest of the Apache uplift (Faulds, 1986).

Provenance from three additional clast count localities parallel the length of Canyon Creek fault to assess variation along depositional strike of the Mogollon Rim Formation (Fig. 13). The southernmost site at Bronson Canyon (BN) is south of Apache paleocanyon and is within its north-flowing Butte Creek paleotributary (Fig. 8). Mazatzal Group (Karlstrom and Conway, 1986) and Hess Canyon rocks, particularly the quartzites, dominate the Bronson Canyon locality. The northernmost site at Steer Ridge (SR), on the Mogollon Rim, is dominated by a variety of older Alder Group crystalline basement rocks, including the distinctive Hells Gate Rhyolite (Conway and Wrucke, 1986); it lacks Paleozoic rocks. The site at Oak Creek Ranch (OC), midway between Steer Ridge (SR) and Bronson Canyon (BN), is composed exclusively of Apache Group rocks.

The distinctly different occurrences in Proterozoic crystalline basement sources between Steer Ridge and Bronson Canyon to the south indicates that two additional ancestral rivers, which sourced different basement terranes, flowed northeastward from the Apache uplift during the Paleogene. The northern of these, here called *Chediski paleocanyon*, is interpreted to have flowed eastward in a path near the present Mogollon Rim (which did not exist at that time). Notably, Steer Ridge (SR) and the inferred Chediski paleocanyon are near the northern end of Canyon Creek fault and accordingly the northern end of the Apache uplift.

A third provenance source is documented as clasts of a suite of volcanic porphyries observed in the Mogollon Rim Formation east of Canyon Creek fault (FV, TF, NC, RT, DC, TC in Fig. 13). The volcanic porphyry clasts are only 1% in the Flying V site and are not found to the north of there. The volcanic porphyry clasts range from 15 to 30% in the other five distal Mogollon Rim Formation localities. This suggests that the Flying V site and other distal sites received gravels from several sources in an alluvial-plain distributary stream network. The volcanic porphyry provenance is clearly a distinct source region separate from those for Apache and Chediski paleocanyons to the north. This distinct provenance supports the probability of a third paleocanyon located south of Apache paleocanyon (Potochnik, 1989). Although not discussed further here, this hypothesized paleocanyon, called *Fort Apache paleocanyon*, was likely separated from Apache paleocanyon by an interfluve here called *Fort Apache upland*. Each of these three subparallel Laramide paleocanyons Chediski, Apache, and Fort Apache, are inferred to be

separated by interfluvial upland regions that contributed tributary and alluvial fan sediments toward their axes.

In its distal northeast outcrops the Mogollon Rim Formation is overlain by fluvial volcaniclastics shed northwestward from the Mogollon-Datil Volcanic Field (Potochnik, 1989). These fluvial volcaniclastic strata are observed at Nash Canyon, Deep Creek, Trout Creek, and Juniper Ridge at or near the Mogollon Rim and range in age from 34 to 18 Ma (Section 5.5.3, Table 1) and will be discussed in the following sections.

5.7. Regional paleocurrents of Mogollon Rim Formation

Clast dispersal was examined at multiple locations north of Apache paleocanyon and west of Canyon Creek fault. From west to east these locations include; Blue Ridge (BR), Tonto Natural Bridge (TB), Buzzard Roost Mesa (BU), Marsh Creek (MC), Bottle Spring (BS), Young Road (YR), Oak Creek Ranch (OC), and Chediski Ridge (CR) (Fig. 14). At Tonto Natural Bridge the column contains no Permian clasts, suggesting the Mogollon Rim did not exist as a prominent topographic feature to the north, as it does today, or that drainage patterns largely excluded clasts from an ancestral rim. Paleocurrent directions are to the southeast and east (Fig. 14), suggesting some local structural or paleotopographic control of Late Eocene streams (Peirce et al., 1979). The mean vector directions for the lower sections of these outcrops show a general easterly distribution with some variance toward the SE and more toward the

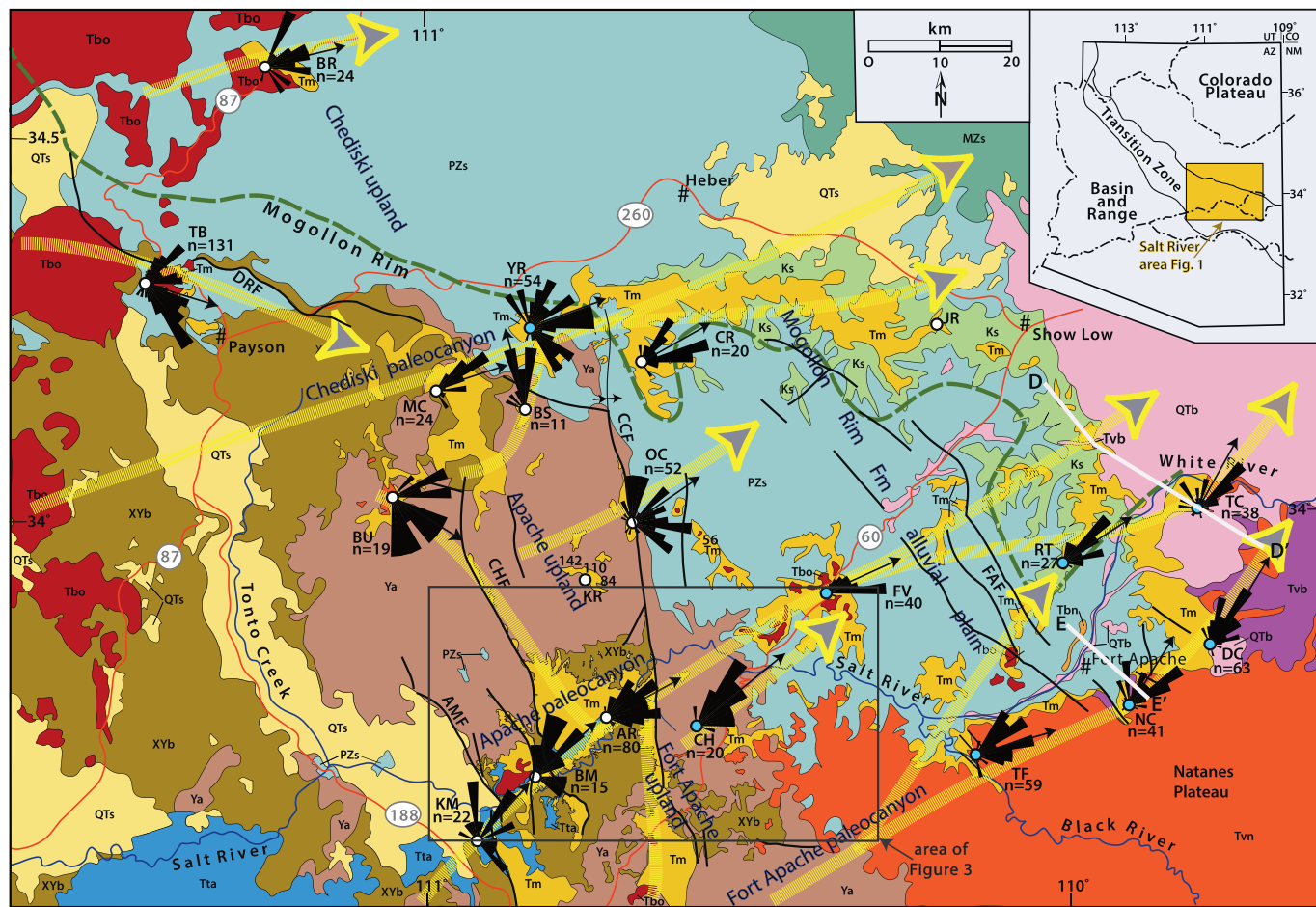


Fig. 14. Paleocurrent rose diagrams of fluvial transport directions of Mogollon Rim sequence (Tm-Tmw) with QTs sedimentary cover partly removed for clarity. Numbers in vicinity of KR are average maximum clast sizes showing diminishment to E-NE (see Potochnik, 1989). Large arrows (in yellow) are generalizations of mean vector directions that show contributary and distributary interpretations of an ancestral deposystem. Ancestral paleogeographic features (blue lettering) are interpretations based on dispersal, provenance, paleotopographic, and geochronologic data. (For interpretation of the references to color in this figure legend, the reader is referred to the web version of this article.)

NE. Maximum clast size (average intermediate diameter in cm) of facies B fanglomerates perched on the now elevated ridges of Keystone Ridge and Oak Creek Ranch show a diminishment toward the east (Fig. 14). East-northeast dispersal directions and absence of Cenozoic basaltic clasts supports the correlation of facies A and B conglomeratic sequences at Blue Ridge and Tonto Natural Bridge (Fig. 12) with the Mogollon Rim sequence.

Dispersal directions of the Mogollon Rim Formation east of Canyon Creek fault are integrated here from the earlier work of Potochnik (1989) where the formation was first described (YR, CH, TF, FV, NC, RT, DC, and TC in Fig. 14). Although some of the original data sets were adjusted with additional data for the purpose of this report, the overall results show the same mean vector directions toward the northeast for the basal conglomerate of the Mogollon Rim Formation. Isopleths of the average maximum clast size (cm) of the basal conglomerate show a northeastward diminishment pattern consistent with the grand mean vector of dispersal for the region east of Canyon Creek fault (Potochnik, 1989). The mean vectors for all east-northeast-dispersed columns are generalized with superimposed yellow vectors to approximate the general trends of three adjacent paleocanyons debouching onto an ancestral alluvial plain (Fig. 14).

5.8. Regional paleocurrents after 33 Ma

Dispersal patterns for streams changed after the ca. 33 Ma close of Mogollon Rim Formation deposition. West of Canyon Creek fault this change is shown in detail for Apache paleocanyon (Figs. 10, 11) and are

summarized in Fig. 15. North of Apache paleocanyon, sections that show drainage reversal in alluvial fan settings include Marsh Creek, Oak Creek Ranch, and Buzzard Roost Mesa. In this interfluve paleogeographic setting drainage patterns reverse to a westerly dispersal direction (Fig. 15).

At Marsh Creek this break is an unconformity that is occupied by a 5-m-thick petrocalcic paleosol composed of chaotically fractured and disrupted, calcite-cemented conglomerate. At Oak Creek Ranch, a basalt flow occupies this interval and has yielded a K-Ar age of 20.62 ± 0.42 Ma (Peirce et al., 1979). At Buzzard Roost Mesa, although this interval is obscured, westward-dispersed fanglomerates above the break are intercalated with a highly potassic mafic flow dated at 25.37 ± 0.09 Ma (Fig. 12, Table 1).

East of Canyon Creek fault this change is shown in the fluvial volcaniclastics overlying the Mogollon Rim Formation near the plateau southern boundary. Paleocurrent measurements of this volcanic-derived region are shown on Fig. 15 at columns labeled Tvs1, Tvs2, and Tvs3 where still preserved beneath younger volcanic fields. The measurements contain a strong signal of flow toward the northwest, with much dispersion in the southernmost site at Nash Canyon (Tvs1). These directions point back to a source in the volcanic terrains of southeastern Arizona and west central New Mexico in contrast to the southwestern, basement-derived provenance from the Mogollon highlands observed in the Mogollon Rim Formation.

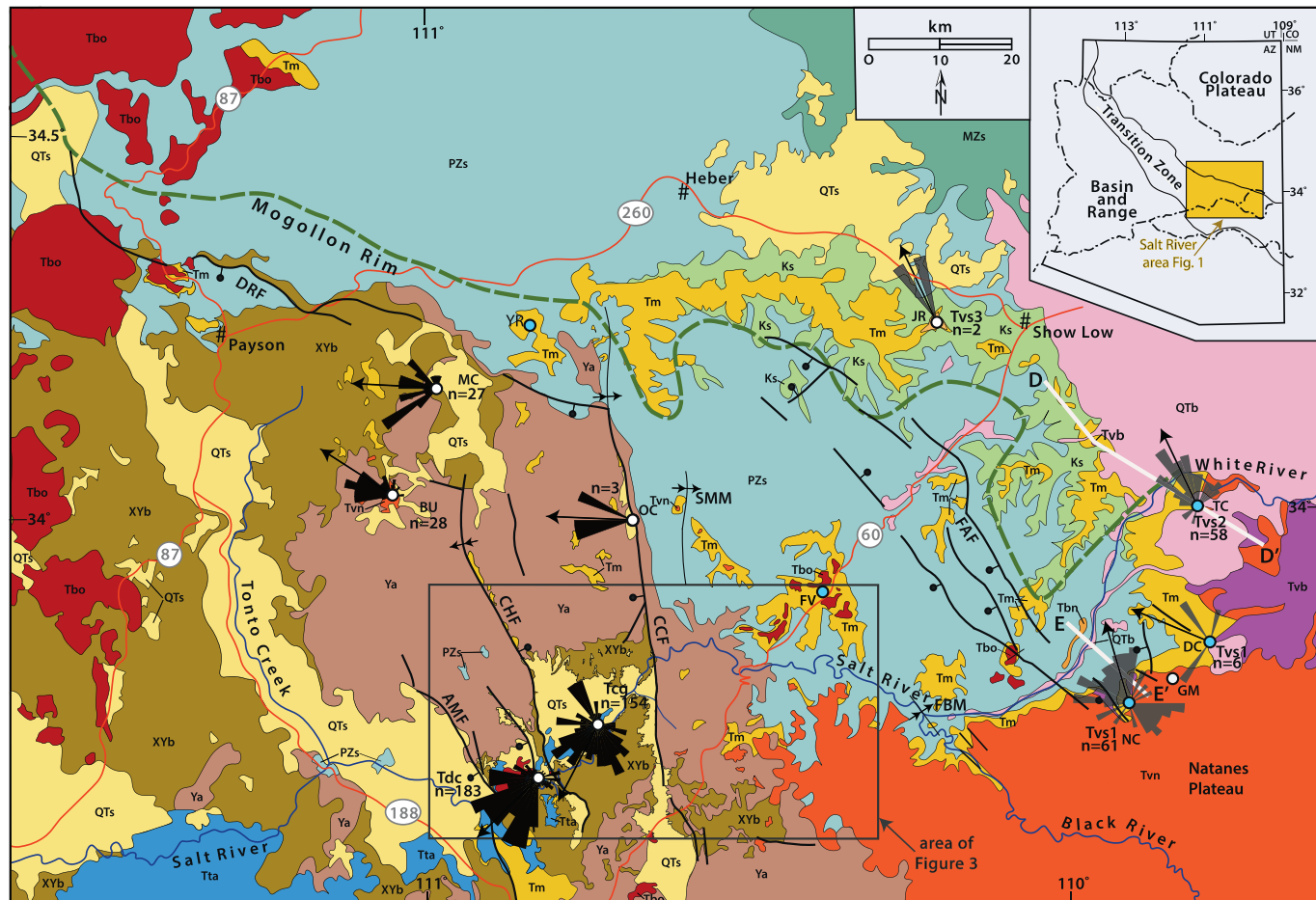


Fig. 15. Paleocurrent rose diagrams of fluvial transport directions following drainage deflection and reversal. Diagrams west of Canyon Creek fault (in black) are for siliciclastic Salt River sequence (QTs). Diagrams east of Canyon Creek fault (in gray) are for Spears Group and subsequent volcaniclastic strata (Tvs1–3). (For interpretation of the references to color in this figure legend, the reader is referred to the web version of this article.)

5.9. Cross sections: geometry of Apache paleocanyon

Detailed geologic mapping and stratigraphic studies permit characterization of the dimensions and shape of Apache paleocanyon. In addition, we studied key geologic structures with an aim toward reconstructing vertical movements across faults and folds through time and how those movements influenced the Cenozoic stratigraphy (Berquist et al., 1981; Faulds, 1986, 1989; Finnell, 1962; Potochnik, 2001a; Potochnik and Faulds, 1998). Below, we summarize key observations in cross sections across and along Apache paleocanyon that show lateral changes in thickness of units.

Three main north-striking fault zones cross Apache paleocanyon, from east to west they are Canyon Creek fault, Cherry Creek fault, and Armer Mountain/Pinal Creek faults. The faults delineate four structural blocks, from east to west: 1) Carrizo block, 2) Apache block, 3) Sierra Ancha block, and 4) Tonto Basin block (Fig. 3). Lines of section A, B, and C are shown in Fig. 3.

5.9.1. Sections A and B: transverse across Apache paleocanyon

Sections A and B are N-S sections perpendicular to the axis of Apache paleocanyon within the Apache and Sierra Ancha blocks, respectively (Fig. 3). Section A traverses the Apache block for about 23 km (13.8 mi.) from north to south rim of Apache paleocanyon (Fig. 16). Here, the topographic relief on the underlying erosion surface from the north rim to the base of the Mogollon Rim sequence along the paleocanyon axis is 1122 m (3682 ft); from the south rim the topographic relief along this surface is 543 m (1780 ft).

Section B (after A-A' in Potochnik and Faulds, 1998) traverses the Sierra Ancha block for about 12 km (7.2 mi.) from north rim to south rim of Apache paleocanyon (Fig. 16). Here, the topographic relief on the underlying erosion surface from the north rim to the base of the Mogollon Rim sequence along the paleocanyon axis is 858 m (2815 ft); from the south rim the topographic relief along this surface is 767 m (2517 ft). North of this section the Proterozoic bedrock of the Sierra Ancha rises unbroken by faults to Aztec Peak, the crest of the Sierra Ancha, at an elevation of 2361 m (7748 ft) (Faulds, 1986; Potochnik, 2001a). Measured from Aztec Peak, the maximum depth of Apache paleocanyon along the trend of B-B' is 1965 m (6448 ft).

5.9.2. Section C: down axis of Apache paleocanyon; Cherry Creek fault-Tonto Basin

Section C follows the axis of Apache paleocanyon from the Apache block westward across the Sierra Ancha block to the Tonto Basin block, illustrating the structural changes from the Transition Zone to the deeply subsided Tonto Basin block (Fig. 17). The Mogollon Rim sequence provides a stratigraphic datum that describes and quantifies faulting after 18.63 Ma deposition of the Apache Leap Tuff. The Sierra Ancha block exhibits an overall eastward tilt of ~10° near the paleocanyon axis (Fig. 17).

The Tonto Basin block is bounded by a headwall breakaway fault zone, Armer Mountain fault (Berquist et al., 1981) and Pinal Creek fault, which accommodate about 1423 m (4669 ft) of down-to-the-southwest offset of the basal Mogollon Rim sequence based on projection of surface mapping. The Dagger Canyon conglomerate exhibits fanning upward dips (Fig. 17), indicating deposition during subsidence and tilting of the Tonto Basin block (Potochnik, 2001a). This relationship and those on the west margin of the Tonto Basin block (Skotnicki, 2002) support an interpretation that the southern Tonto Basin is primarily a half-graben bounded on its east flank by a listric normal fault system that was active after emplacement of Black Mesa basalt (14.84 Ma). Continuation of the Dagger Canyon depositional system across part of the southern Tonto Basin is evident Anderson et al., 2021). Ten degree eastward tilting of the Sierra Ancha block (Fig. 17) may be due to a concave-upward geometry of the Coon Creek fault and/or footwall uplift at the eastern margin of the Tonto Basin.

5.10. Cross sections: thickness variations of the Mogollon Rim Formation and subsequent incision near the plateau margin

Sections D and E (Figs. 18, 19) parallel the Mogollon Rim on the Colorado Plateau boundary near its eastern terminus, where it is covered by three temporally discrete volcanic provinces that exhibit a complex set of stratigraphic relationships (Fig. 1): 1) Mogollon-Datil (37.6–18.6 Ma; McIntosh and Chamberlain, 1994); 2) Mount Baldy (9.8–8.7 Ma; Damon et al., 1996; Merrill and Pewe, 1977); and 3) Springerville (3.00–0.60 Ma; (Anderson et al., 2021); Condit and Shafiqullah, 1985; Condit and Connor, 1996; Damon et al., 1996) (Figs. 1, 2). These volcanic provinces preserve stratigraphic details of Cenozoic depositional

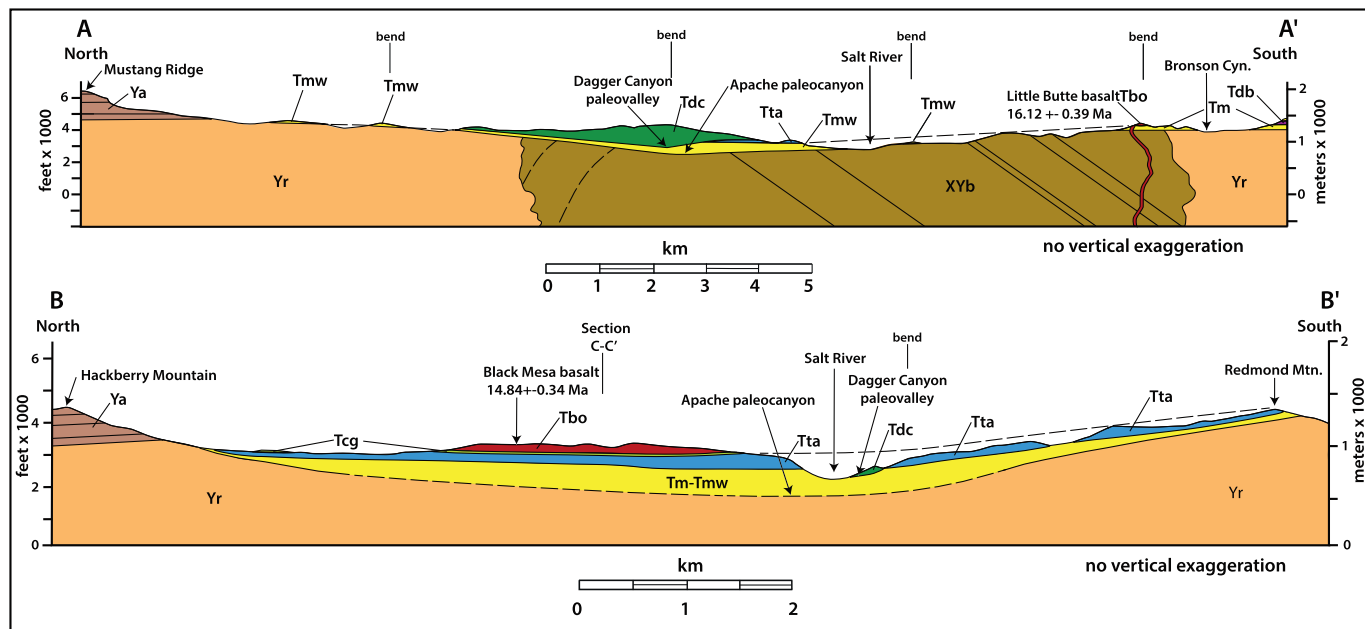


Fig. 16. Sections A and B are transverse to modern Salt River and Laramide Apache paleocanyon within Apache and Sierra Ancha blocks, respectively (Fig. 3). Apache paleocanyon and inset Dagger Canyon paleovalley depths can be assessed in these sections (see Section 5.9.1 in text).

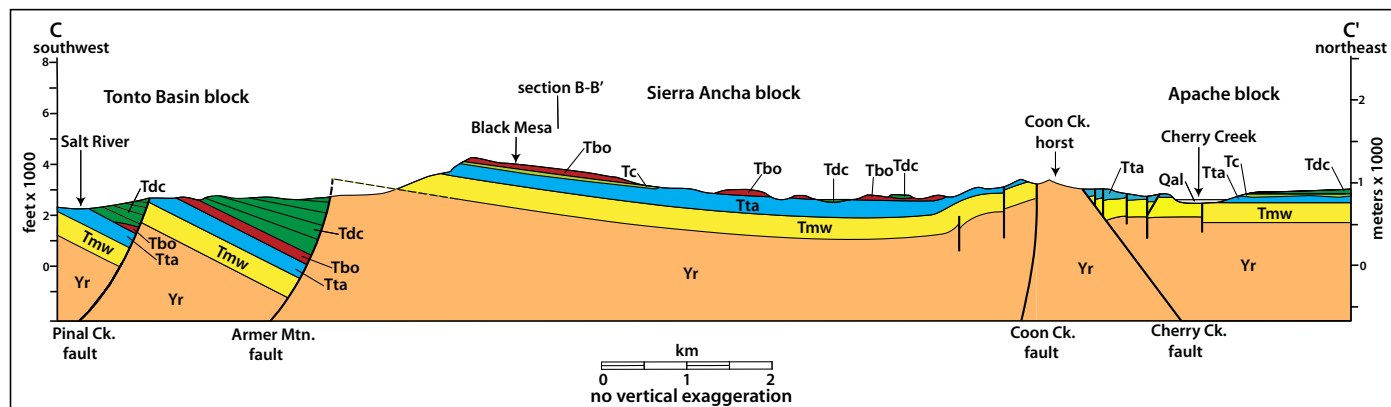


Fig. 17. Section C is axial to Salt River depositional system from Tonto Basin to Apache block (Fig. 3). Cherry Creek fault is a basement-cored, west-facing Laramide monoclinal with opposite sense reactivation during structural collapse of the Apache uplift (Faulds, 1989). Coon Creek horst is vantage point for Fig. 5 photo. Armer Mountain and Pinal Creek faults are breakaway listric normal faults for southern Tonto Basin with concurrent deposition of Dagger Canyon Conglomerate, illustrating base level fall to the southwest during drainage reversal (Potochnik, 2001a). Eastward tilt of Black Mesa is ascribed to footwall uplift of Armer Mountain-Pinal Creek faults and/or listric rotation of Coon Creek fault.

and erosional systems, defined by unconformities between the volcanic provinces, and the dispersal of volcanic-sedimentary sequences represented by each system. Lines of section D and E are shown on Fig. 1.

Section D displays paleogeographic details ranging in age from the Late Cretaceous to the present (Fig. 18). The Permian Kaibab Formation was beveled prior to marine deposition of the Late Cretaceous Dakota Sandstone (K1 in Fig. 2). The Dakota was in turn beveled prior to deposition of the Round Top Mtn and Mogollon Rim Formations (T1, T2 in Fig. 2). Section D illustrates southeast thickening of the Mogollon Rim Formation, from a thin veneer of rim gravels on the northwest to more than 400 m where the formation projects beneath the volcanic fields to the southeast. This thickening reflects the greatest thickness of the Mogollon Rim Formation along the northeastern projection of Apache paleocanyon.

Section D illustrates the complex aggradation/degradation episodes during volcanic-clastic sedimentation 33–18.6 Ma (T3a–T3c in Fig. 2). The attenuation of the “rim gravels” at its northwestern end suggests the possibility of a paleotopographic low area on the Mogollon Rim that may have accommodated Late Miocene stream flow from the north (T4 in Fig. 2). In addition, there appears to be an ancestral Pliocene paleovalley incised into the Mount Baldy volcanics and underlying rocks. This Pliocene paleovalley is infilled by a thin veneer of Dagger Canyon Conglomerate (T5 in Fig. 2) overlain by Plio-Pleistocene volcanic rocks of the Springerville volcanic field.

Section E crosses the modern White River south of Section D near the confluence of the North and East Forks (Fig. 1). It shows the progressive mid to late Cenozoic incision history of the modern Salt River in its upper reaches south of the Mogollon Rim (Fig. 19). In this section a flow remnant from the Mount Baldy volcanic complex is deeply inset against the Late Eocene Tvs1 volcaniclastic conglomerates, defining the T4 erosion surface. In turn, the 3.0 Ma basalt of the elongate Nan Dahs Taan Mesa (Tbn, Fig. 1; White River mesa basalt of Anderson et al., 2021) parallels the modern White River and is more deeply inset at a lower elevation. This elongate basalt-capped mesa overlies a residual outcrop of Dagger Canyon Conglomerate 275 m above the modern White River thalweg and defines the T5 erosion surface. A 0.6 Ma basalt flow emplaced along the Quaternary course of the North Fork at its modern elevation defines the T6 erosion surface. Together, these cross sections reveal a long term geomorphic history of the southern Colorado Plateau margin since the Eocene, leading to the modern Salt River drainage.

6. Discussion

6.1. Laramide fluvial and eolian systems

A key context for Cenozoic stratigraphy and paleotopography in the southwest is that Laramide orogenesis was followed by a period of intense erosion and landscape leveling during middle Cenozoic time. This interval of erosion beveled Laramide structures, including monoclines and other folds on the Colorado Plateau and in the Transition Zone (Potochnik, 1989), as well as thrust faults, folds, and other structures in the Basin and Range Province (Scarborough, 1989). Erosion regionally removed kilometers of rocks, bringing Proterozoic rocks and Laramide and older plutons to the surface over broad areas of the Transition Zone and Basin and Range Provinces. This event produced an erosion surface called the “Late Eocene erosion surface” (Epis and Chapin, 1975) or more generally “Rocky Mountain erosion surface” (Abbott and Cook, 2012; Gresans, 1981) across much of the western U.S. In much of the northern Cordillera, the Rocky Mountain erosion surface produced regions of relatively low, beveled relief (Cather et al., 2012; Potochnik and Damon, 1986) but it resulted in locally high relief closer to Laramide mountains, including near the ancestral Mogollon highlands (Beard and Faulds, 2011; Faulds, 1989; Young and Hartman, 2011).

The Round Top Mountain formation fluvial redbeds exhibit a stratigraphic position, Mogollon highland basement provenance, and northeastward dispersal direction that mark a Paleogene system that eroded Cenomanian Dakota Group marine rocks and beveled Laramide monoclines east of Canyon Creek fault (Potochnik, 1989, 2001b). Deep oxidation of these sediments suggests correlation with profound climatic warming in the Early to Middle Eocene (Zachos et al., 2008). Round Top Mountain formation is lithostratigraphically correlated with the Eocene Baca Formation in New Mexico (Cather et al., 1994).

The overlying Late Eocene Mogollon Rim Formation records a regional, through-going, northeast-flowing drainage system from ancestral highlands in the Transition Zone of central Arizona to lowlands in the Colorado Plateau region of northern Arizona. The basal Mogollon Rim sequence west of Canyon Creek fault correlates eastward with the Mogollon Rim Formation based on stratigraphic position, proximity, age, sedimentology, dispersal patterns, and provenance. As such, the coeval Whitetail Formation is here included as headland proximal facies in a regional lithosome of a northeast-flowing integrated fluvial depositional system that ranges from bedrock highlands to alluvial plains (Fig. 14). Well-rounded quartzite boulders as large as 2 to 5 m in diameter in the basal Mogollon Rim Formation at Flying V support an interpretation of a renewed pulse of Mogollon highland uplift in the Late Eocene

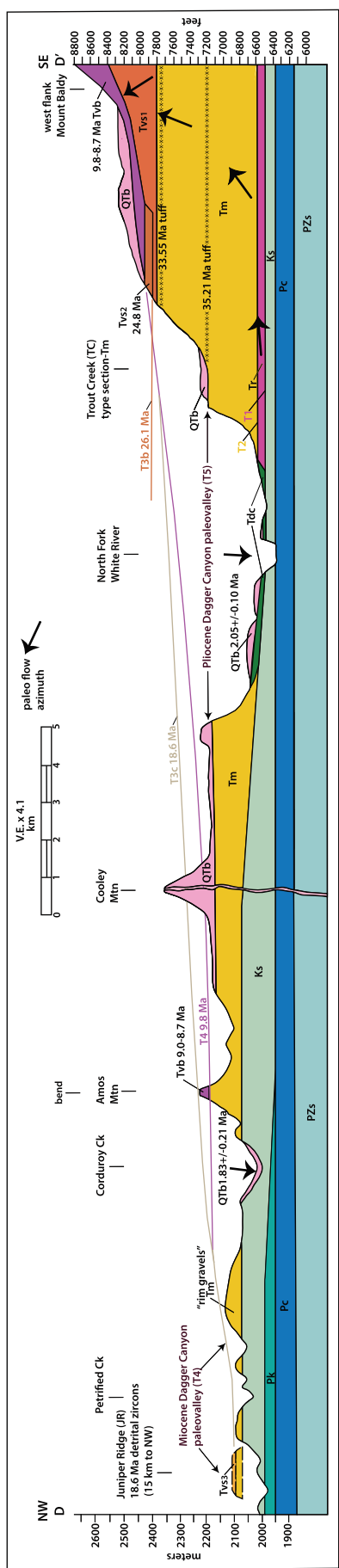


Fig. 18. Section D parallels the Mogollon Rim and cuts across the upper White River into the west flank of the Mount Baldy volcanic complex, view toward N30°E (**Fig. 1**). Stratigraphic relationships of the three temporally discrete volcanic/clastic sequences (Tvs1–3, **Fig. 2**) bury the Mogollon Rim Formation and show stratigraphic relationships to the “rim gravel” lag deposits of today. Note erosional level of Permian Kaibab Formation and Cretaceous marine strata, both coincident with the Mogollon Rim Formation type section at Trout Creek. Tvs3 volcaniclastic veneer on rim gravels at Juniper Ridge northwest of this section represents the last phase of Mogollon-Datil volcaniclastic sedimentation northwestward toward the Little Colorado River Basin ca. 18.6 Ma. Proposed ancestral Miocene paleovalley incised into the Mogollon Rim, 13.7–7.7 Ma, is hypothesized for Lake Hopi spillover and incision of Dagger Canyon paleovalley after 14.84 Ma. Dagger Canyon Conglomerate is deposited in a Pliocene paleovalley incised into 8.7 Ma Mount Baldy mafic outflow sheets preserved at Amos Mountain; and, is overlain by early Pleistocene basalt flows from the Springerville Volcanic Field.

(Potochnik, 1989). The Mogollon Rim Formation is coeval and correlative with the fluvial Eagar Formation (Sirrine, 1958; Witcher et al., 1994) in easternmost Arizona and possibly the Deza Member at the base of the Chuska Sandstone in the Four Corners region (Cather et al., 2008). The Mogollon Rim Formation deposystem occupies Apache paleocanyon incised into the Laramide Mogollon highland up to 1965 m in depth prior to aggradation beginning before 37.6 Ma. This stream system likely continued eastward toward the Laramide Baca Basin in west-central New Mexico and perhaps to the Gulf of Mexico (Cather et al., 2008).

A modern analogue for this scenario is the South Platte River as it transects the Front Range of the Rocky Mountains near Denver, CO. Here, a modern drainage originates in the topographically highest ranges of the central Rocky Mountains then crosses eastwardly a major range-bounding fault before becoming an alluvial plain stream on the Great Plains to the Mississippi River. Similarly, the Cache la Poudre to the north and Arkansas River to the south parallel the South Platte on their journey to the Mississippi River. These central Rocky Mountain streams have not undergone subsequent extensional tectonism as has the southeastern Colorado Plateau in this study but do invite modern comparisons for the Eocene Mogollon Rim Formation streams.

The bedrock erosion surface beneath the Mogollon Rim Formation is certainly much older than the basal conglomerate that overlies it. Volcanic cobbles sampled from the basal conglomerate at Round Top Mountain on the Mogollon Rim are dated as young as 54 Ma (Peirce et al., 1979). Detrital sanidine and zircon populations sampled from the basal conglomerate at Flying V range from 59 to 64 Ma (Anderson et al., 2021). These Round Top Mountain and Flying V clasts are the same age range as Laramide intrusive rocks in the Globe Miami mining district source region to the southwest (Potochnik, 1989). These clast ages and the average maximum clast size of the Mogollon Rim Formation basal conglomerate across the region (Potochnik, 1989), together with paleocurrent patterns and provenance (Sections 5.6, 5.7), suggest a single alluvial plain sequence deposited on a broad erosion surface carved prior to 54 Ma.

East of Canyon Creek fault, the alluvial plain received deposition of the litharkosic sand-dominated facies A of the Mogollon Rim Formation ca. 40–33 Ma. As mid-Tertiary extension encroached on the region, fluvial sediments became structurally trapped by down-to-the-west normal-sense reactivation of Canyon Creek (**Fig. 8**) and Fort Apache fault zones (Potochnik, 1989). Consequently, the ancestral alluvial plain became increasingly starved of sediment from the waning northeast-flowing streams 33–25 Ma. A well-developed petrocyclic soil formed on the upper surface of the Mogollon Rim Formation alluvial plain prior to widespread deposition of mafic volcanic flows of the Natanes Plateau and adjacent surfaces 24.76–20.62 Ma. On the southern margin of the Colorado Plateau at about 33 Ma, waning northeastward surface streams merged with northwestward-dispersed fluvial volcaniclastic aprons distributed from the newly emerging calderas of the Mogollon-Datil volcanic highlands (**Figs. 15, 18**).

Climatic cooling at about 34 Ma (Zachos et al., 2008) is temporally associated with the Chuska Erg 33.5 to ~27 Ma over a large region north and east of this study area (Cather et al., 2008). Late Eocene fluvial dispersal northeastward from the Mogollon highland toward the Baca Basin was probably blocked, absorbed, and/or deflected by eolian and volcaniclastic deposition during the Oligocene. The light colors, upward fining and temporal correlation of uppermost Mogollon Rim Formation (Potochnik, 1989) with the onset of the Chuska Erg are indicative of climatic drying in the region. The transport capacity of streams was likely reduced by cooling/aridification of the Oligocene climate, when northeastward stream dispersal patterns on the southern Colorado Plateau margin show north and northwestward deflection (**Fig. 15**). It is apparent that onset of Chuska eolian deposition ca. 33.5 Ma (Cather et al., 2008) and Mogollon-Datil ignimbrite volcanism ca. 34 Ma (McIntosh and Chamberlain, 1994) both influenced the evolution of stream systems following Eocene time.

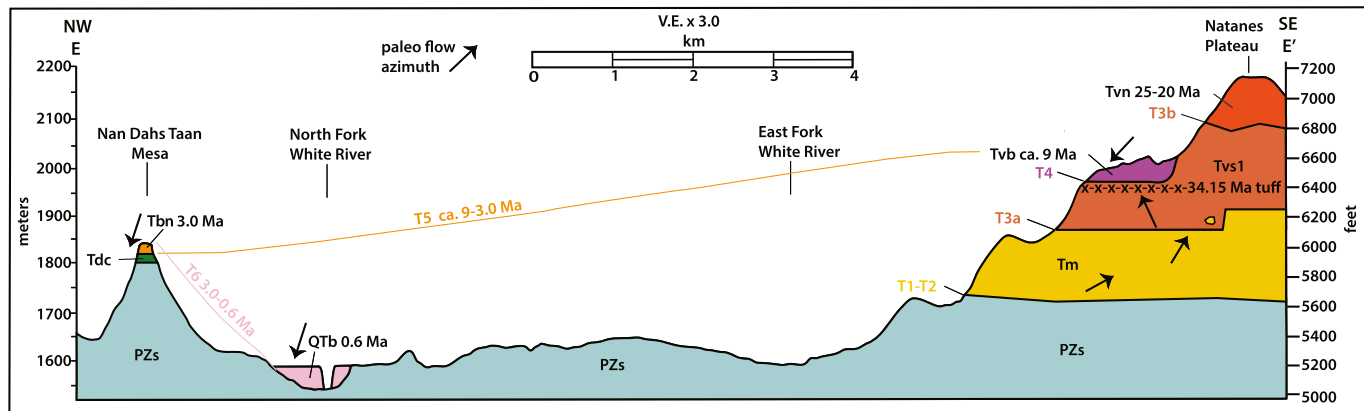


Fig. 19. Section E parallels the Mogollon Rim southwest of Section D and bisects the upper White River a short distance upstream of the confluence of North and East Forks (Fig. 1). Note stratigraphic evidence for progressive southwestward incision of the White River (upper Salt River) following emplacement of Early Miocene Natanes Plateau basalt. Mount Baldy (ca. 9 Ma), Nan Dahs Taan (3.0 Ma), and Springerville (0.6 Ma) volcanic flows show progressive incision of the region by Dagger Canyon and ancestral Salt River streams (T4–6 in Fig. 2).

6.2. Emergence of the Mogollon-Datil volcanic highlands

Oligocene-Early Miocene northwest-flowing streams sourced in the Mogollon-Datil volcanic highlands of western New Mexico were responsible for deposition of up to 977 m of fluvial volcaniclastic and eolian, mostly fine-grained tuffaceous sediments as documented in the Alpine1/Federal geothermal corehole at the Alpine Divide (Witcher et al., 1994) and adjacent Escudilla Mountain near the AZ-NM border east of this study area (Cather et al., 2008). These sediments, including fluvial Spears Group and eolian Chuska Sandstone, gradationally overlie 331 m of Eager Formation in the corehole. The Eager is stratigraphically equivalent to 375 m of the correlative Mogollon Rim Formation at Trout Creek (Fig. 18). Aggradation of this thick sedimentary pile on the western flank of the emerging Mogollon-Datil volcanic field by northwest-flowing streams and eolian sand dunes marks a profound change in stream dispersal from northeast to northwest on the southern margin of the Colorado Plateau. Deposition of the volcaniclastic Spears Group began in this area with accumulation of the 34.2 Ma Tvs1 unit (NC in Fig. 15) and may have continued until widespread emplacement of andesite lavas at 26.1 Ma in western New Mexico (Bearwall Mountain Andesite in McIntosh and Chamberlain, 1994).

A modern analogue for this Oligocene setting is the Yellowstone caldera complex at the crest of the Rocky Mountains in Wyoming. Here, a nested Quaternary caldera complex highland on the northern continental divide generates three major rivers that radiate from its center; Missouri, Snake, and Green River systems. Similarly, the Mogollon-Datil is a nested Oligocene caldera complex on the southern continental divide that is the source region for three major rivers that radiate from its center; Gila, Little Colorado, and Rio Grande River systems. From this comparison it appears that emplacement of large volumes of felsic magma at shallow crustal levels in an intracontinental setting can have a profound and enduring influence on the origin of radial drainage networks.

The Tertiary section at the Alpine1/Federal corehole in addition to the adjacent Escudilla Mountain section are projected laterally to Fig. 21 as an hypothetical maximum original thickness that conceivably could have existed on the Mogollon Rim at ca. 26.1 Ma. Subsequent erosion of this thick sedimentary sequence occurred over the period 26.1 to ca. 16 Ma, as bracketed by the Bearwall Andesite in western New Mexico and basal Bidahochi Formation (Fig. 20) in northern Arizona (Dallege et al., 2003; Douglass et al., 2020) (Table 1). Cather et al. (2008) quantified this profound degradational episode as at least 1210 m of Oligocene-Early Miocene erosion between the Chuska Mountains and the basal contact of the Bidahochi Formation along the axis of the Little Colorado River (Figs. 20, 21). This erosional episode at the Mogollon

Rim eroded the Spears Group, Chuska Sandstone, and most of the Mogollon Rim Formation. Northwest-flowing streams from the Mogollon-Datil volcanic highlands (Tvs2, Tvs3 in Fig. 15) may have stripped up to 1292 m from the Mogollon Rim at Juniper Ridge (Fig. 21). These erosional episodes are defined by the unconformities within the sequence as T3b and T3c (Figs. 2, 18).

During this erosional episode, the Early Miocene Natanes Plateau basalts (Tvn) were emplaced over an extensive region east of Canyon Creek fault and south of the Mogollon Rim ca. 25–20 Ma (Fig. 15). The Spears Group (Tvs1) was not deposited in the region west of Nash Canyon (NC in Fig. 15) indicating the ancestral Mogollon highland continued to serve as a topographic high 34–26.1 Ma. Local SW-down reversal on Canyon Creek fault was underway prior to 25.7 Ma emplacement of the Buzzard Roost basalt (BU in Figs. 12, 15). In the region between Canyon Creek fault and Mogollon Rim a petrocalcic soil developed on the largely abandoned Mogollon Rim Formation alluvial plain surface ca. 33–25 Ma. Emplacement of the Natanes Plateau volcanic field was mostly to the south and west and apparently did not extend onto the Colorado Plateau, suggesting southward flexure of the Transition Zone after ca. 25 Ma (Potocznik, 1989).

Despite southwestward structural flexure in the Transition Zone, persistence of northwest-flowing streams from the Mogollon Datil region continued onto the southern Colorado Plateau into the Middle Miocene as evidenced by the Fence Lake Formation (Lucas and Anderson, 1994) in western New Mexico and similar Tvs2 and Tvs3 volcanics at Trout Creek and Juniper Ridge (Fig. 15). The Tvs3 Juniper Ridge volcaniclastic outcrop which, overlies basal lag gravel of the Mogollon Rim Formation on the Mogollon Rim, can be no older than the 18.6 ± 2.7 Ma from the detrital zircon population in the deposit (Potocznik et al., 2012) (Table 1). This zircon population is similar to the eruption age of the Superstition cauldron to the southwest, not the older Mogollon Datil cauldrons to the east. These zircons may have arrived in the Tvs3 Juniper Ridge outcrop on the Mogollon Rim by fluvial or eolian transport. Regardless of transport mechanism, the fluvial volcaniclastic veneer on the basement-derived rim gravels at Juniper Ridge provide an important signal for the cessation of northwest flowing streams that governed fluvial systems on the southern Plateau boundary ca. 34.15–18.6 Ma. These northwest-flowing ancestral streams exposed a broadly eroded, low relief landscape of Paleozoic and Mesozoic strata prior to deposition of the Bidahochi Formation beginning ca. 16 Ma (Dallege et al., 2003; Douglass et al., 2020).

Based on the stratigraphic evidence for successive erosion of volcaniclastic rocks from the southern Plateau region, the Little Colorado River valley of today is largely a relic landscape of Oligocene-Early Miocene aggradation and subsequent degradation by northwest-

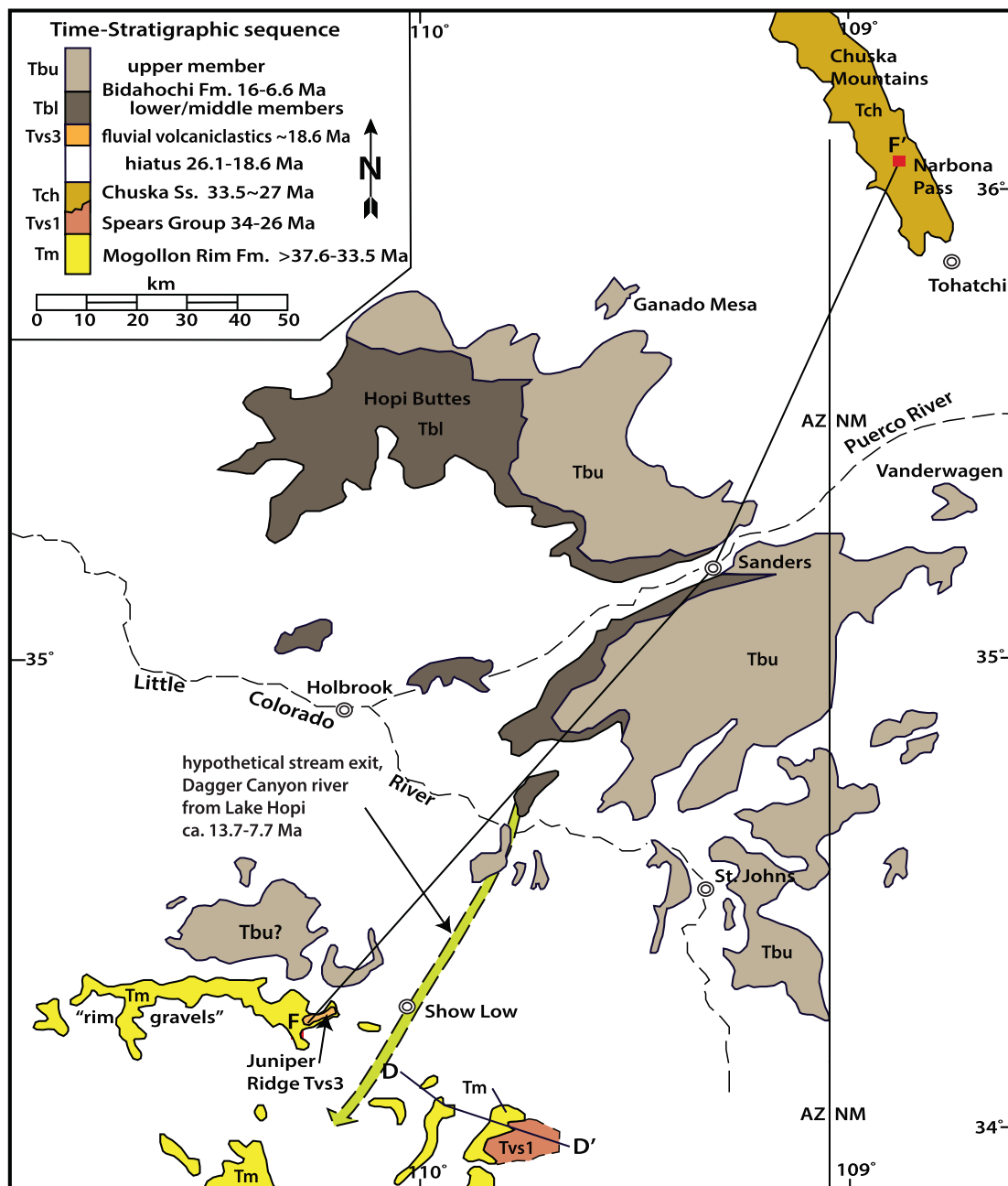


Fig. 20. Map of upper Little Colorado River basin shows distribution of Bidahochi Formation (ca. 16–6.6 Ma) deposited on ancestral Little Colorado River erosion surface that had been stripped of earlier Cenozoic sediments. Area of map is shown in Fig. 22. Hypothetical spillover path southward from ancestral Lake Hopi (lower Bidahochi Fm) across Mogollon Rim illustrates possible water source for Dagger Canyon paleovalley/river, ca. 13.7–7.7 Ma (Figs. 18, 19). Lithic designators are same as Fig. 2 except Tch (eolian Chuska Sandstone), Tbl, Tbu (lower and upper Bidahochi Formation) are shown in inset stratigraphic column.

flowing streams. Northeastward limitation of these streams may have been controlled by erosional scarp retreat of underlying Mesozoic strata. The outlet for this northwest stream system may have been through an ancestral eastern Grand Canyon (Fig. 22) (Flowers and Farley, 2012; Karlstrom et al., 2014, 2017; Scarborough, 2001) that may have been incised to the top of the Mississippian Redwall Limestone (Lee et al., 2013; Sears, 2013). Mid-Cenozoic sedimentary basins in the Lake Mead region west of the Colorado Plateau are possible depocenters (Faulds et al., 2016; Lamb et al., 2010, 2018). Alternatively, far-reaching Miocene fluvial connections with the northwestern U.S. (Sears, 2013) although possible, require a subsequent continental scale drainage reversal scenario. These postulations are testable with provenance studies that could link the Mogollon-Datil volcaniclastic-bearing streams

with a Middle Miocene depocenter via the ancestral Little Colorado River paleogeographic linkage.

6.3. Late Miocene Basin and Range subsidence

Within Apache paleocanyon, the Whitetail facies of the Mogollon sequence (Figs. 2, 7) aggraded due to several forcing factors prior to 18.63 Ma. Structural reversal of Laramide faults and structural tilting toward the southwest (Potochnik, 1989) appear to gradually decrease stream gradient of northeast-flowing streams. Regional aridification in the Oligocene would have increased hillslope sediment yield to paleotopographic low areas while reducing axial stream power. Eruption of Natanes Plateau basalt flows hindered waning northeast-flowing

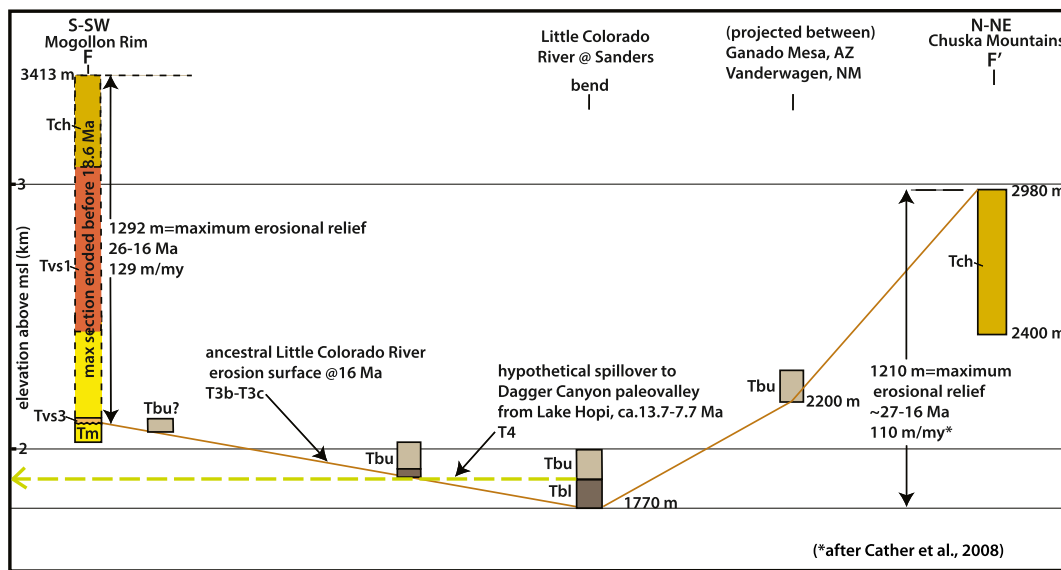


Fig. 21. Section F, Mogollon Rim to Chuska Mountains across Little Colorado River basin. Depicts profile of ancestral Little Colorado River valley, defined from base of Bidahochi Formation to top of Early Oligocene fluvial and eolian sediments. Maximum possible deposition of Tm/Tvs1/Tch sediments (Mogollon Rim Formation, Spears Group, and Chuska Sandstone) projected to Mogollon Rim from Alpine1/Federal corehole shows the greatest possible thickness of sediments deposited then eroded prior to 16 Ma. Hypothesized 13.7–7.7 Ma stream spillover from Lake Hopi is shown. Lithic designators as in Figs. 2, 20.

streams. These factors indicate that a once vigorous axial stream had lost most of its competency and capacity within Apache paleocanyon, causing aggradation in a bedrock paleocanyon setting.

Southwestward structural subsidence of the Transition Zone following deposition of the Mogollon Rim Formation is well-documented (Faulds, 1986, 1989; Finnell, 1962; Potochnik, 1989; Potochnik and Faulds, 1998). Structural collapse of the Laramide Mogollon highland was underway by 25.4 Ma (BU in Fig. 12). High dispersion of northward paleocurrent measurements along the Butte Creek paleotributary parallel to Canyon Creek fault suggest west side down reactivation of the fault during aggradation of the Whitetail facies (Fig. 8). Nonetheless, paleocurrent directions of the locally sourced Whitetail facies indicate that diminished streamflow continued northeastward through Apache paleocanyon until emplacement of the Superstition cauldron tuffs ca. 18.63 Ma (Fig. 9). Initial drainage reversal toward the southwest within Apache paleocanyon from 18.63–14.84 Ma occurred in a partly ponded basin with weakly expressed alluvial fans and playas of the Chalk Creek Formation (Fig. 10), not unlike the Great Basin of today.

Following this 4 million year period of drainage ponding and internal drainage, the “geologically sudden” appearance of a renewed, erosive, and more regionally-integrated southwest-flowing stream was initiated across the Apache uplift within the bedrock confines of Apache paleocanyon. This stream incised the Dagger Canyon paleovalley at least 366 m into pre-existing paleocanyon fill and was subsequently infilled with 276–453 m of the Dagger Canyon Conglomerate (Figs. 5, 7, 11). Incision of this ancestral paleovalley into basalt flows as young as 14.84 Ma by a southwest flowing stream indicates a newly introduced discharge of surface water from the northeast and an increase in stream gradient. The Dagger Canyon stream carved its paleovalley during the period between 14.84 Ma basalt emplacements and deposition of 7.1 Ma detrital siltstones in the upper Dagger Canyon Conglomerate (Fig. 7) (Anderson et al., 2021). This 7.7 million year hiatus roughly coincides with the onset of Basin and Range extension in the Tonto Basin that would have induced a base level fall to the southwest and deposition of the lower conglomerate facies in the Tonto Basin (Faulds, 1989; Nations, 1988). In this scenario, base level fall induces headward erosion that progressively migrates to the northeast 52–90 km to the modern Mogollon Rim, increasing its watershed and stream power during the 7.7 m.y. period.

An alternative (but not exclusive) driver for drainage reversal is a ponding and overflow scenario from the southern Colorado Plateau margin (Potochnik, 2011; Scarborough, 1989, 2001). Spillover from the Bidahochi Formation basin (ancestral Lake Hopi) is indirectly inferred from stratal accumulation rates, facies changes, and an apparent hiatus in Member 4 (Dallege et al., 2003; Douglass et al., 2020). Stratal accumulation rates decrease by over 400% to 7 m/Ma after 13.7 Ma with deposition of lacustrine Member 3. Granule conglomerate occurs in Member 4, suggesting fluvial transport across the basin. The next younger age from the upper Member 4 is 7.7 Ma. This profound slowing of the deposition rate over a 6 m.y. period suggests throughflow in the basin that predates outflow through Grand Canyon (Douglass et al., 2020). A hypothetical outflow from the Bidahochi Basin is to the south where the Dagger Canyon paleovalley incised into pre-existing canyon fill after 14.84. A modern analogue for this scenario is Lake Victoria and the origin of the White Nile River in the uplifted continental rift system of east Africa. Lake Victoria is a very large and shallow lake ponded on an uplifted continental plateau province between two sub-parallel, offset arms of the East Africa Rift (Reader, 2001). This modern setting is broadly analogous to the southeastern Colorado Plateau province that is also an uplifted intracontinental plateau bounded on the east by the Rio Grande rift and on the south by the southern Basin and Range province.

How does a stream that has reached a local base level extend itself to a lower region nearer to regional base level? This question is addressed in various regional studies (e.g. Douglass et al., 2020; Larson et al., 2017). It is also addressed in a study of the small catchment geomorphic system in Grand Canyon of the Colorado River (Thompson et al., 2000). This investigation of late Holocene river sand bars concluded that local base level in small ephemeral tributary catchments may be exceeded by three processes: ponding/overflow, alluvial fan progradation, and piping/surface collapse. Observations at 119 catchments concluded that one or some combination of these three mechanisms led to downstream integration of the ephemeral stream and consequent rapid headward erosion. In this late Holocene model, headward erosion is the *result* of downstream integration, not the *cause*. If we consider that “the small mirrors the large”, we postulate that these three geomorphic mechanisms, alone or in combination, are drivers for the origin of Dagger Canyon paleoriver. This proposed model provides a ground for future

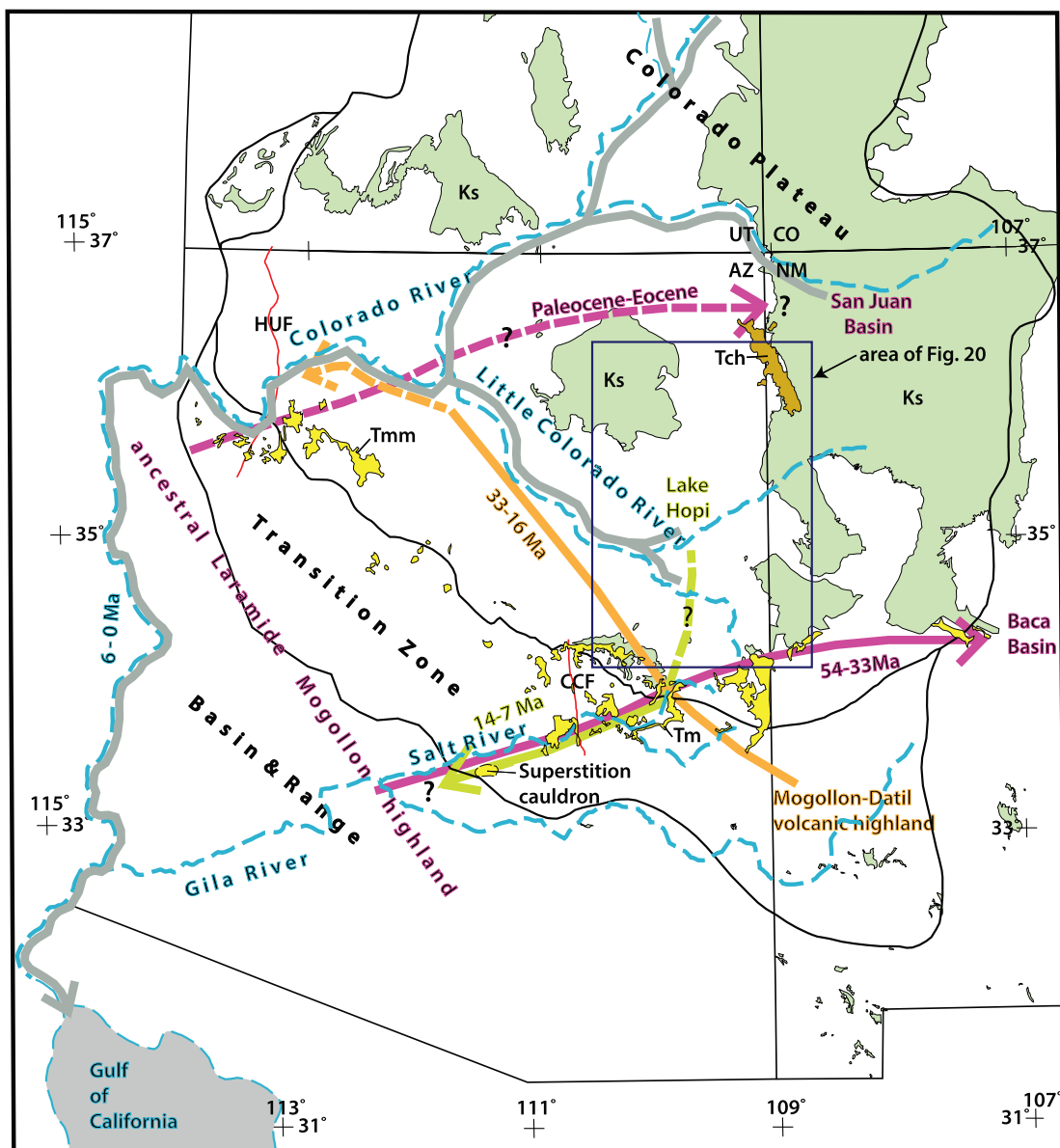


Fig. 22. Source to sink paleogeographic model of Cenozoic drainage evolution across Colorado Plateau southern boundary based on this report. Upper Cretaceous marine Dakota Sandstone (in green) provides approximate sea level planation template for reference. Primary uplifts, dispersal directions, and possible depocenters are shown. Locations and lithic designators as in Figs. 1, 2, except Tmm-Music Mountain Formation, HUF-Hurricane fault. (For interpretation of the references to color in this figure legend, the reader is referred to the web version of this article.)

research on this important paleo geomorphic question.

The southwest-flowing Dagger Canyon paleoriver (Fig. 5) may have traversed the Transition Zone region prior to structural subsidence of Tonto, Higley, Luke and other basins of the southern Basin and Range province. Its path may have joined the Gila River trough of today (Fig. 22). It remains an open question as to whether the Dagger Canyon/Gila paleoriver reached as far as the Pacific Ocean. The Eocene-Miocene Sespe marine delta along the California coast contains quartzite clasts similar to the Troy Quartzite and White Ledges Formation (Howard, 2000), widely exposed in Apache paleocanyon walls (Karlstrom et al., 2020). It is possible their provenance may be from the Dagger Canyon paleovalley. The Dagger Canyon river had sufficient stream power and time (broadly 14.8–7.1 Ma) to travel through existing water gaps to the Pacific Ocean (e.g. San Gorgonio Pass near Banning, CA). In this hypothetical scenario, the Dagger Canyon paleoriver originates in ancestral Lake Hopi on the Colorado Plateau and follows a path to the ancestral Sespe basin north of Los Angeles, CA. This stream path may have utilized

preexisting paleocanyons through the structurally-collapsing ancestral Mogollon highland to reach the Pacific Ocean prior to opening of the Gulf of California ca. 6 Ma (Oskin and Stock, 2003). That aside, southwestward thickening and fanning dips of the Dagger Canyon Conglomerate (Fig. 17) indicates that Dagger Canyon paleovalley fill was influenced by progressive collapse of the Tonto Basin

Interruption and blockage of the Dagger Canyon river from ancestral Lake Hopi may have been due to footwall uplift of the Mogollon Rim rift shoulder during Basin and Range extension. If so, surface waters of ancestral Lake Hopi would have been shunted westward toward the paleo eastern Grand Canyon exit point (Douglass et al., 2020; Karlstrom et al., 2014, 2017; Scarborough, 2001) during deposition of the upper fluvial member of the Bidahochi Formation ca. 6 Ma. In this scenario, spillover of Bidahochi Formation surface waters would have switched from south to west, resulting in integration of the modern Colorado River through ancestral eastern Grand Canyon and ultimately to the Gulf of California after 6 Ma (Fig. 22).

Progressive incision of the modern Salt River near the Mogollon Rim is constrained by emplacement of ca. 9 Ma Mount Baldy volcanic flows, the 3.00 Ma basalt of Nan Das Taan mesa, and more recent Quaternary basalt flows (Fig. 19). A Mount Baldy flow remnant (ca. 9–8 Ma) is inset against earlier Cenozoic strata above the modern East Fork of White River (Fig. 2, T4). The Nan Das Taan basalt flow, further inset, is a linear, elongate mesa that parallels the modern North Fork of the White River and is perched about 275 m above the modern thalweg. It overlies a thin veneer of well-rounded basement-derived gravels of probable Dagger Canyon Conglomerate (Fig. 19). The source of this basalt flow is likely from the Plio-Pleistocene Springerville Volcanic Field on the Colorado Plateau. This indicates that outflow sheets of basalt from the Mount Baldy volcanic field at Amos Mountain were breached by the Pliocene North Fork of White River by 3.00 Ma (Fig. 18). Subsequent basalt flows bled southward over the Mogollon Rim into existing tributaries of the upper Salt River from 2.05 to 0.60 Ma (Figs. 18, 19; Table 1).

Progressive incision of the modern Salt River in the Apache paleocanyon (Fig. 16) is constrained by the inset Dagger Canyon Conglomerate and more deeply inset Plio-Pleistocene strath terraces. The Dagger Canyon Conglomerate aggraded 337 m to an elevation of 1313 m within the Dagger Canyon paleovalley and is capped by a red-brown mollisol (Fig. 5). The greatest thickness of Dagger Canyon Conglomerate is in the east tilted Armer Mountain fault block (Fig. 17). Greater thicknesses of Dagger Canyon conglomerate are likely buried beneath more recent basin fill farther west in the Tonto Basin (Anderson et al., 2021; Nations, 1988). The mollisol paleosol surface on the upper Dagger Canyon conglomerate provides a datum that constrains subsequent incision by the modern Salt River in the region west of Canyon Creek fault.

The modern Salt River canyon thalweg coincides with the axis of Apache paleocanyon and Dagger Canyon paleovalley at Canyon Creek fault but is superimposed parallel and south of these axes as it crosses the Apache uplift/graben (Figs. 8, 11). The modern Salt River incises a steep-walled gorge into the south wall of Apache paleocanyon composed of resistant, steeply tilted Early Proterozoic metavolcanic and metasedimentary rocks of the Redmond Formation and Hess Canyon Group (Fig. 3). The stratigraphic record of broad scale cutting and filling episodes that define the Cenozoic geologic history is mostly preserved along the north flank of the modern Salt River within the Apache uplift (Potocznik, 2001a; Skotnicki, 2002). Distinctive Pleistocene terraces along the length of the Salt River west of Canyon Creek fault (Faulds, 1986, 1989; Potocznik, 2001a) and intracanyon Pleistocene basalt flows east of Canyon Creek (Condit and Shafiqullah, 1985; Anderson et al., 2021) demonstrate that the modern Salt River had achieved its present course and profile by late Pliocene to early Pleistocene time.

7. Summary

Data presented here are consistent with the following summary of Cenozoic drainage reversal in east-central Arizona. Fig. 22 illustrates a paleogeographic source to sink model that extends westward to the Grand Canyon region. As such, this study provides constraints that may be relevant, in some measure, to the paleogeographic development of the mainstem Colorado River region to the west (Fig. 22). A summary chronology follows:

- 1) East-northeast-flowing early Laramide streams (Paleogene) from the uplifted ancestral Mogollon highland beveled gently northeast-tilted sedimentary rocks ranging in age from Late Cretaceous to Late Proterozoic from a large region south of the Colorado Plateau. Fine-grained fluvial red beds (Round Top Mountain formation) from this period remain in broadly scattered localities across the region and may correlate with the Baca Formation in west-central New Mexico.
- 2) A renewed pulse of Eocene uplift induced incision of a paleocanyon network up to 1965 m deep into the uplifted ancestral Mogollon highland between ca. 54 and 37 Ma. The Apache uplift is a 27 km-

wide, north-trending Laramide upthrown block bounded by outwardly vergent high angle reverse faults/monoclines in the eastern part of the Mogollon highlands. Two, possibly three east-northeast oriented bedrock paleocanyons (Chediski, Apache, and Fort Apache) were incised across the Apache uplift. These canyons delivered arkosic sands and gravels east-northeast across Canyon Creek fault via powerful streams onto the ancestral alluvial plain of the Mogollon Rim Formation.

- 3) With normal-sense reactivation of the bounding faults, the Apache uplift within the Mogollon highland began a slow structural collapse into a graben from ca. 25.4 to 18.6 Ma, reducing stream competence, and inducing aggradation of the Whitetail facies within Apache paleocanyon and on adjacent interfluvial uplands. Weak northeast streamflow continued until emplacement of the regionally extensive Apache Leap Tuff at 18.63 Ma. This emplacement marked both the end of northeast stream flow and onset of a period of sluggish drainage reversal (Chalk Creek Formation) within Apache paleocanyon until 14.84 Ma deposition of basalt flows on the paleocanyon fill.
- 4) In the Mogollon Rim area to the northeast, emergence of the Mogollon-Datil volcanic field induced northwest stream flow from its volcanic aprons 34.2–26.1 Ma, mixing with and overwhelming arkosic basement-derived sediments from the ancestral Laramide Mogollon highland. Contemporaneous aggradation of the Oligocene Chuska erg 33–27 Ma signaled further disruption of northeast flowing streams. Initially a blanket of fluvio-eolian sediments aggraded on the southern plateau margin up to 1292 m in thickness (Mogollon Rim/Eager Formations, Spears Group, Chuska Sandstone) during this arid period of caldera volcanism in the Oligocene. Subsequently, progressive erosion by northwest-flowing streams apparently stripped nearly all of these sediments from the southern Colorado Plateau margin, laying bare the erosion surface that received the Bidahochi Formation ca. 16 Ma. Widespread basalts of the Natanes Plateau blanketed the region south and east of the Colorado Plateau margin ca. 25 to 20 Ma between episodes of fluvial volcanoclastic deposition, transport, and erosion. Northwest streamflow waned by 18.6 Ma, leaving a thin veneer of fluvial mixed-source gravels of the Fence Lake Formation and its correlatives. The outlet for northwest-flowing streams from ca. 25–18.6 Ma may have been through ancestral eastern Grand Canyon, which had been carved to sufficient depth to allow surface waters to emerge west of the Kaibab Plateau toward a yet to be defined depocenter. The lengthy period of northwest streamflow and erosion sculpted the essential outline of the modern Little Colorado River valley, setting the stage for ponding of local streams in the Middle Miocene Lake Hopi (lower Bidahochi Formation 16–7 Ma).
- 5) Within Apache paleocanyon to the southwest, previously deposited sedimentary and volcanic rocks were deeply incised by a southwest-flowing stream at 14.84 Ma, forming the Dagger Canyon paleovalley. The paleovalley, 366 m deep, is inset within the bedrock confines of Apache paleocanyon. The timing of Dagger Canyon stream incision coincides with profoundly slowing deposition rate in ancestral Lake Hopi from 13.7 to 7.7 Ma, suggesting a spill outlet to the south that may have incised the Dagger Canyon paleovalley. The ancestral paleovalley may have predated Tonto Basin, allowing for southwest-flowing surface waters to connect with the Gila River drainage for a roughly 6 m.y. period. The ancestral Gila may have reached the Pacific Ocean in the delta of the Sespe Formation. Blockage of this hypothesized Colorado Plateau outlet appears to be northward flexure of the plateau margin, forcing southern plateau surface waters toward a paleo Grand Canyon outlet and establishment of the Colorado River main stem of today.
- 6) Between the Mogollon Rim and Canyon Creek fault, progressive incision of the White-Salt River drainage is defined by successively younger and lower inset Late Miocene-Quaternary basalt flow remnants ca. 9–0.6 Ma. Plateau uplift is inferred to be the cause of

- progressive incision of the upper Salt River Basin and Range down faulting of the Tonto Basin and other basins southwest of this area contributed to base level fall that enhanced incision after 14.84 Ma. The Dagger Canyon paleovalley was refilled with >337 m of southwest-distributed Dagger Canyon Conglomerate likely due to cutoff of source water and base level fall in Tonto Basin. The modern Salt River was superimposed and progressively incised into all Apache paleocanyon fill during the Pliocene-Pleistocene, establishing its modern course 3.00–0.60 Ma.
- 7) The Cenomanian Dakota Formation K1 transgression provides an initial sea level reference surface upon which all subsequent stream systems were emplaced during the Cenozoic Era. The source to sink paths of ancestral and modern streams on the southern Colorado Plateau boundary region are, in part, relic features of ancestral stream courses initially established in Paleogene to Miocene time. Paleotopography, ponding/spillover, superposition, and headward erosion acted in concert to govern the origin and evolution of modern Salt River drainage patterns.

Declaration of competing interest

We have no competing interests and our funding sources had no involvement in the decision to publish this work.

Acknowledgments

The knowledge of the late H. Wesley Peirce and Paul E. Damon inspired the early phases of this work. We have benefitted much from discussions with R.A. Young, S.M Cather, J.D. Nations, and W.R. Dickinson. Stephen J. Reynolds was instrumental in providing financial support and intellectual guidance for the successful completion of this work. W.C. McIntosh, P.E. Damon, and M. Shafiqullah conducted radiometric analyses. Sue Beard provided logistical and editorial support to bring this to print. Constructive reviews by two anonymous individuals and Karl E. Karlstrom significantly improved this paper. Funding was from the National Science Foundation (EAR-9206055 and EAR-9417901), the American Chemical Society, and the Michael Engl Family Foundation. We are grateful to the White Mountain Apache Tribe for allowing access to their lands and to the Tonto National Forest Salt River team, Don Sullivan and Brian McCormick, for assisting with Salt River access.

Appendix A. Supplementary data

Supplementary data associated with this article can be found in the online version, at <https://doi.org/10.1016/j.geomorph.2022.108286>. These data include the Google Earth map of important areas described in this paper.

References

- Abbott, L., Cook, T., 2012. Geology Underfoot along Colorado's Front Range. Mountain Press Publishing Company, Missoula, Montana.
- Anderson, J.L., 1989. Proterozoic orogenic granites of the southwestern United States. In: Jenney, J.P., Reynolds, S.J. (Eds.), Geologic Evolution of Arizona. Arizona Geological Society Digest, 17, pp. 211–233.
- Anderson, J.C., Karlstrom, K.E., Heizler, M.T., 2021. Neogene drainage reversal and Colorado Plateau uplift in the Salt River area, Arizona, USA. *Geomorphology* 395. <https://doi.org/10.1016/j.geomorph.2021.107964>.
- Beard, L.S., Faulds, J.E., 2011. Kingman uplift, paleovalleys and extensional foundering in northwest Arizona. In: Beard, L.S., Karlstrom, K.E., Young, R.A., Billingsley, G.H. (Eds.), CRevolution 2-Origin and Evolution of the Colorado River System, Workshop Abstracts. U.S. Geological Survey Open-File Report 1210, pp. 28–37.
- Berquist, J.R., Shrider, A.F., Wrucke, C.T., 1981. Geologic map of the Sierra Ancha Wilderness and Salome study area, Gila County, Arizona. In: U.S. Geological Survey Miscellaneous Field Studies Map, MF-1162A.
- Bull, W.B., 1972. Recognition of alluvial-fan deposits in the stratigraphic record. *SEPM Spec. Publ.* 16, 63–83.
- Cather, S.M., Johnson, B.D., 1984. Eocene tectonics and depositional setting of west-central New Mexico and eastern Arizona. In: New Mexico Bureau of Mines and Mineral Resources Circular, 192, 33 p.
- Cather, S.M., Chamberlin, R.M., Ratte, J.C., 1994. Cenozoic stratigraphy and nomenclature for western New Mexico and eastern Arizona. In: Chamberlin, R.M., Kues, B.S., Cather, S.M., Barker, J.M., McIntosh, W.C. (Eds.), New Mexico Geological Society 45th Annual Field Conference Guidebook, pp. 259–266.
- Cather, S.M., Connell, S.D., Chamberlin, R.M., McIntosh, W.C., Jones, G.E., Potochnik, A.R., Lucas, S.G., Johnson, P.S., 2008. The Chuska erg: paleogeomorphic and paleoclimatic implications of an Oligocene sand sea on the Colorado Plateau. *Geol. Soc. Am. Bull.* 120, 13–33. <https://doi.org/10.1130/B26081.1>.
- Cather, S.M., Chapin, C.E., Kelley, S.A., 2012. Diachronous episodes of Cenozoic erosion in southwestern North America and their relationship to surface uplift, paleoclimate, paleodrainage, and paleoaltimetry. *Geosphere* 8, 1177–1206. <https://doi.org/10.1130/GES00801.1>.
- Chamberlin, R.M., Harris, J.S., 1994. Upper Eocene and Oligocene volcaniclastic sedimentary stratigraphy of the Quemado-Escondido Mountain area, Catron County, New Mexico. In: New Mexico Geological Society Guidebook, 45th Field Conference, pp. 269–275.
- Cobban, W.A., Hook, S.C., 1984. Mid-Cretaceous molluscan biostratigraphy and paleogeography of southwestern part of Western Interior, United States. In: Westermann, G.E.G. (Ed.), Jurassic-Cretaceous Biochronology and Paleogeography of North America. Geological Association of Canada, Special Paper 27, pp. 257–271.
- Condit, C.D., Connor, C.B., 1996. Recurrence rates of volcanism in basaltic volcanic fields: an example from the Springerville volcanic field, Arizona. *Geol. Soc. Am. Bull.* 108 (10), 1225–1241. [https://doi.org/10.1130/0016-7606\(1996\).108.10.1225.RR](https://doi.org/10.1130/0016-7606(1996).108.10.1225.RR).
- Condit, C.D., Crumpler, L.S., Aubele, J.C., 1994. Thematic geologic maps of the Springerville volcanic field, east-central Arizona. In: U.S. Geological Survey, Miscellaneous Series Investigation Map I-2431, Scale 1:100,000.
- Condit, C.D., Shafiqullah, M., 1985. In: K-Ar Ages of Late Cenozoic Rocks of the Western Part of the Springerville Volcanic Field, East-central Arizona. Isochron West, No. 44, pp. 3–5.
- Conway, C.M., Wrucke, C.T., 1986. Proterozoic geology of the Sierra Ancha-Tonto basin-Mazatzal Mountains area, road log and fieldtrip guide. In: Arizona Geological Society Digest, v. 16, pp. 237–238.
- Conway, C.M., Silver, L.T., 1989. Early Proterozoic rocks (1710–1615 Ma) in central to southeastern Arizona. In: Jenney, J.P., Reynolds, S.J. (Eds.), Geologic Evolution of Arizona. Arizona Geological Society Digest, 17, pp. 165–186.
- Cooley, M.E., Davidson, E.S., 1963. The Mogollon highlands-their influence on Mesozoic and Cenozoic erosion and sedimentation. In: Arizona Geological Society Digest, v. 6, pp. 7–35.
- Crumpler, L.S., Aubele, J.C., Condit, C.D., 1994. Volcanoes and neotectonic characteristics of the Springerville volcanic field, Arizona. In: New Mexico Geological Society Guidebook, 45th Field Conference, pp. 147–164.
- Cuffney, R.G., 1976. Geology of the White Ledges Area, Gila County, Arizona. Colorado School of Mines, Golden.
- Dallege, T.A., Ort, M.H., McIntosh, W.C., 2003. Mio-Pliocene chronostratigraphy, basin morphology and paleodrainage relations derived from the Bidahochi Formation, Hopi and Navajo Nations, northeastern Arizona. *Mt. Geol.* 40 (3), 55–82.
- Damon, P.E., Shafiqullah, M., Harris, R.C., Spencer, J.E., 1996. Compilation of Unpublished Arizona K-Ar Dates From the University of Arizona Laboratory of Isotope Geochemistry, 1971–1991. Arizona Geological Survey Open-File Report, OFR-96-18.
- Darton, N.H., 1925. A Resume' of Arizona Geology: Arizona Bureau of Mines Bulletin, 119, 298p.
- Davis, G.H., Showalter, S.R., Benson, G.S., McCalmont, L.S., Faulds, J.E., Cropp, F.W., 1982. The Apache uplift, heretofore unrecognized Colorado Plateau uplift. *Geol. Soc. Am. Abstr. Programs* 14, 472–473.
- Doe, M.F., Jones III, J.V., Karlstrom, K.E., Thrane, K., Frei, D., Gehrels, G., Pecha, M., 2012b. Basin formation near the end of the 1.60–1.45 Ga tectonic gap in southern Laurentia: Mesoproterozoic Hess Canyon Group of Arizona and implications for ca. 1.5 Ga supercontinent configurations. *Lithosphere* 4 (1), 77–88.
- Dorn, R.I., Skotnicki, S.J., Wittmann, A., Van Soest, M., 2020. Provenance in drainage integration research: case studies from the Phoenix metropolitan area, south-Central Arizona. *Geomorphology* 371. <https://doi.org/10.1016/j.geomorph.2020.107430>.
- Douglass, J.C., Gootee, B.F., Dallegge, T., Jeong, A., Seong, Y.B., Yu, B.Y., 2020. Evidence for the overflow origin of the Grand Canyon. *Geomorphology* 369. <https://doi.org/10.7361/j.geomorph.2020>.
- Epis, R.C., Chapin, C.E., 1975. Geomorphic and tectonic implications of the post-Laramide, late Eocene erosion surface in the southern Rocky Mountains. *Geol. Soc. Am. Mem.* 144, 45–74.
- Faulds, J.E., 1986. Cenozoic Geologic History of the Salt River Canyon Region, Gila County, Arizona [M.S. thesis]. University of Arizona, Tucson, 319 p.
- Faulds, J.E., 1989. Geologic map of the Salt River region, Rockin straw Mountain quadrangle. In: Arizona Geological Survey Contributed Map CM-89-B, Scale 1: 24,000.
- Faulds, J.E., Schreiber, B.C., Langenheim, V.E., Hinz, N.H., Shaw, T.H., Heizler, M.T., Perkins, M.E., El Tabakh, M., Kunk, M.J., 2016. Paleogeographic implications of late Miocene lacustrine and nonmarine evaporite deposits in the Lake Mead region: immediate precursors to the Colorado River. *Geosphere* 12 (3), 721–767.
- Ferguson, C.A., Trapp, R.A., 2001. Stratigraphic nomenclature of the Miocene Superstition Volcanic Field, central Arizona. In: Arizona Geological Survey Open File Report, OFR-01-06, 103 p.
- Finnell, T.L., 1962. Recurrent movement on the Canyon Creek fault, Navajo County, Arizona. In: U.S. Geological Survey Professional Paper 450-D, pp. 80–82.

- Finnell, T.L., 1966a. Geologic map of the Chediski Peak quadrangle, Navajo County, Arizona. In: U.S. Geological Survey Geologic Quadrangle Map GQ-544, Scale 1: 62,500, 1 Sheet.
- Finnell, T.L., 1966b. Geologic map of the Cibque Quadrangle Map, Navajo County, Arizona. In: U.S. Geological Survey Geologic Quadrangle Map GQ-545, Scale 1: 62,500, 1 Sheet.
- Flowers, R.M., Farley, K.A., 2012. Apatite $^{40}\text{He}/^{3}\text{He}$ and $(\text{U}-\text{Th})/\text{He}$ evidence for an ancient Grand Canyon. *Science* 338, 1616–1619, 101126/science.1299390.
- Gresans, R.L., 1981. Extension of the Telluride erosion surface to Washington state, and its regional and tectonic significance. *Tectonophysics* 79, 145–164.
- Howard, J.L., 2000. Provenance of quartzite clasts in the Eocene-Oligocene Sespe Formation: paleogeographic implications for southern California and the ancestral Colorado River. *Geol. Soc. Am. Bull.* 112, 1635–1649. [https://doi.org/10.1130/0016-7606\(2000\)112<1635:POQCIT>2.0.CO;2](https://doi.org/10.1130/0016-7606(2000)112<1635:POQCIT>2.0.CO;2).
- Karlstrom, K.E., Conway, C.M., 1986. Deformational styles and contrasting lithostratigraphic sequences within an Early Proterozoic orogenic belt, central Arizona. In: Nations, J.D., Conway, C.M., Swann, G.A. (Eds.), *Geology of Central and Northern Arizona*. Geological Society of America, Rocky Mountain Section, Guidebook, pp. 1–25.
- Karlstrom, K.E., Lee, J., Kelley, S., Crow, R., Crossey, L.J., Young, R., Lazear, G., Beard, L.S., Ricketts, J., Fox, M., Shuster, D., 2014. Formation of the Grand Canyon 5 to 6 million years ago through integration of older palaeocanyons. *Nat. Geosci.* <https://doi.org/10.1038/ngeo2065>, 74 p.
- Karlstrom, K.E., Crossey, L.J., Embid, E., Crow, R., Heizler, M., Hereford, R., Beard, L.S., Ricketts, J.W., Cather, S., Kelley, S., 2017. Cenozoic incision history of the Little Colorado River: its role in carving Grand Canyon and onset of rapid incision in the past ca. 2 MA in the Colorado River System. *Geosphere* 13 (1), 49–81. <https://doi.org/10.1130/GES01304.1>.
- Karlstrom, K.E., Jacobson, C.E., Sundell, K.E., Eyster, A., Blakey, R., Ingwersoll, R.V., Mulder, J.A., Young, R.A., Beard, L.S., Holland, M.E., Shuster, D.L., Winn, C., 2020. Evaluating the Shinumo-Sespe drainage connection: arguments against the “old” (70–17 Ma) Grand Canyon models for Colorado Plateau drainage evolution. *Geosphere* 16 (6), 1425–1456. <https://doi.org/10.1130/GES02265.1> (2020).
- Krieger, M.H., Johnson, M.G., Biggsby, P.R., 1979. Mineral resources of the Aravaipa Canyon Instant Study Area, Pinal and Graham Counties, Arizona. In: U.S. Geological Survey Open-File Report 79-291, 27 p.
- Lamb, M.A., Martin, K.L., Hickson, T.A., Umhoefer, P.J., Eaton, L., 2010. Stratigraphy and age of the lower Horse Spring Formation in the Longwell Ridges area, southern Nevada: Implications for tectonic interpretations. In: Umhoefer, P.J., Beard, L.S., Lamb, M.A. (Eds.), Miocene Tectonics of the Lake Mead Region, Central Basin and Range: Geological Society of America Special Paper 463, pp. 171–201. [https://doi.org/10.1130/2010.463\(08\)](https://doi.org/10.1130/2010.463(08)).
- Lamb, M.A., Beard, L.S., Dragos, M., Hanson, A.D., Hickson, T.A., Sitton, M., Umhoefer, P.J., Karlstrom, K.E., Dunbar, N., McIntosh, W., 2018. Provenance and paleogeography of the 25–17 Ma Rainbow Gardens Formation: evidence for tectonic activity at ca. 19 Ma and internal drainage rather than throughgoing paleorivers on the southwestern Colorado Plateau. *Geosphere* 14 (4). <https://doi.org/10.1130/01127.1>. CR-02-A.
- Larson, P.H., Dorn, R.I., Douglass, J., Gootee, B.F., Arrowsmith, R., 2010. Stewart Mountain Terrace: a new Salt River terrace with implications for landscape evolution of the lower Salt River Valley, Arizona. *J. Ariz. Nev. Acad. Sci.* 42, 26–36.
- Larson, P.H., Meek, N., Douglass, J., Dorn, R., Seong, Y.B., 2017. How rivers get across mountains: transverse drainages. *Ann. Am. Assoc. Geogr.* 107 (2), 274–283.
- Larson, P.H., Dorn, R.I., Skotnicki, S.J., Seong, Y.B., Jeong, A., DePonty, J., 2020. Impact of drainage integration on basin geomorphology and landform evolution: a case study along the Salt and Verde rivers, Sonoran Desert, USA. *Geomorphology* 371. <https://doi.org/10.1016/j.geomorph.2020.107439>.
- Lee, J.P., Stockli, D.F., Kelley, S.A., Pederson, J.L., Karlstrom, K.E., Ehlers, T.A., 2013. New thermochronometric constraints on the Tertiary landscape evolution of the central and eastern Grand Canyon, Arizona. *Geosphere* 9 (2), 216–228. <https://doi.org/10.1130/GES00842.1>.
- Livingston, D.E., 1969. Geochronology of Older Precambrian Rocks in Gila County, Arizona [Ph.D. thesis]. University of Arizona, Tucson, 224 p.
- Lucas, S.G., Anderson, O.J., 1994. Miocene proboscidean from the Fence Lake Formation, Catron County, New Mexico. In: Chamberlin, R.M., Kues, B.S., Cather, S.M., Barker, J.M., McIntosh, W.C. (Eds.), New Mexico Geological Society 45th Annual Field Conference Guidebook. New Mexico Geological Society, Inc, pp. 277–278.
- Lucchitta, I., 1979. Late Cenozoic uplift of the southwestern Colorado Plateau and adjacent lower Colorado River region. *Tectonophysics* 61, 63–95. [https://doi.org/10.1016/0040-1951\(79\)90292-0](https://doi.org/10.1016/0040-1951(79)90292-0).
- McIntosh, W.C., Chamberlain, R.M., 1994. 40Ar/39Ar geochronology of middle to late Cenozoic ignimbrites, mafic lavas, and volcaniclastic rocks in the Quemado region, New Mexico. In: Chamberlin, R.M., Kues, B.S., Cather, S.M., Barker, J.M., McIntosh, W.C. (Eds.), New Mexico Geological Society 45th Annual Field Conference Guidebook. New Mexico Geological Society, Inc, pp. 165–173.
- McIntosh, W.C., Ferguson, C.A., 1998. Sanidine, single crystal, laser-fusion 40Ar/39Ar geochronology database for the Superstition Volcanic Field, central Arizona. In: Arizona Geological Survey Open-File Report OFR-98-27, 74 p.
- McKay, E.J., 1972. Geologic map of the Show Low quadrangle, Navajo County, Arizona. In: U.S. Geological Survey Geologic Quadrangle Map GQ-973, Scale 1:62,500, 1 Sheet.
- Merrill, R.K., Pewe, T.L., 1977. Late Cenozoic geology of the White Mountains, Arizona. *Ariz. Bureau Geol. Miner. Tech. Spec. Pap.* 1, 65 p.
- Molenaar, C.M., 1983. Major depositional cycles and regional correlations of Upper Cretaceous rocks, southern Colorado Plateau and adjacent areas. In: Reynolds, M.W., Dolly, E.D. (Eds.), Mesozoic Paleogeography of West Central United States, Rocky Mountain Paleogeography Symposium 2. Society of Economic Paleontologists and Mineralogists, pp. 201–224.
- Moore, R.T., Peirce, H.W., 1967. Geologic map of the Fort Apache Indian Reservation, Arizona. Ariz. Bur. Mines Bull 177.
- Nations, J.D., 1988. Stratigraphy and tectonic significance of Cenozoic basin-fill sediments, Tonto Basin, Arizona. In: Anderson, L., Piety, L. (Eds.), *Field Trip Guidebook to the Tonto Basin, Friends of the Pleistocene Fall Fieldtrip*, pp. 165–186.
- Oskin, M., Stock, J., 2003. Pacific-North America plate motion and opening of the Upper Delfin basin, northern Gulf of California, Mexico. *Geol. Soc. Am. Bull.* 115, 1173–1190. <https://doi.org/10.1130/B25154.1>.
- Peirce, H.W., 1982. Cenozoic Drainage Reversal in the Mogollon Rim Area - A Classic Example: Unpublished Paper Presented at the 35th Annual Symposium on Southwestern Geology, Museum of Northern Arizona, Flagstaff.
- Peirce, H.W., 1984. The Mogollon escarpment. *Ariz. Bureau Geol. Miner. Tech. Fieldnotes* 14 (2), 8–11.
- Peirce, H.W., Damon, P.E., Shaqullah, M., 1979. An Oligocene (?) Colorado Plateau edge in Arizona. *Tectonophysics* 61, 1–24.
- Peterson, D.W., 1969. Geologic map of the Superior Quadrangle, Pinal County, Arizona. In: U.S. Geological Survey GQ-818.
- Potochnik, A.R., 1989. Depositional style and tectonic implications of the Mogollon Rim formation (Eocene), east-central Arizona. In: Anderson, O.J., Lucas, S.G., Love, D.W., Cather, S.M. (Eds.), New Mexico Geological Society 40th Annual Field Conference Guidebook, pp. 107–118.
- Potochnik, A.R., 2001a. Cenozoic Structural and Paleogeographic Evolution of the Transition Zone, Central Arizona [Ph.D. thesis]. Arizona State University, Tempe, 173 p.
- Potochnik, A.R., 2001b. Paleogeomorphic evolution of the Salt River region: implications for Cretaceous-Laramide inheritance for ancestral Colorado River drainage. In: Young, R.A., Spamer, E.E. (Eds.), *Colorado River Origin and Evolution, Grand Canyon Association*, Monograph No. 12, pp. 17–22.
- Potochnik, A.R., 2011. Ancestral Colorado River exit from the Plateau Province-Salt River hypothesis [M.S. thesis]. In: Beard, L.S., Karlstrom, K.E., Young, R.A., Billingsley, G.H. (Eds.), *CRevolution 2—Origin and Evolution of the Colorado River System, Workshop Abstracts: U.S. Geological Survey Open-File Report 2011–1210*, 319 p. <http://pubs.usgs.gov/of/2011/1210/>.
- Potochnik, A.R., Damon, P.E., 1986. Tectonic and geomorphic implications of post-Laramide erosion. *Geol. Soc. Am. Abstr. Programs* 18, 403.
- Potochnik, A.R., Faulds, J.E., 1998. A tale of two rivers: Cenozoic structural inversion and drainage reversal across the southern boundary of the Colorado Plateau. In: Duebendorfer, E.M. (Ed.), *Geologic Excursions in Northern and Central Arizona: Field Trip Guidebook for Geological Society of America Rocky Mountain Section Meeting*, pp. 149–173.
- Potochnik, A.R., Dickinson, W.R., Pecha, M., 2012. Mogollon Rim gravels, detrital zircon evidence for north-northwest-flowing early Miocene streams during exhumation of the Chuska Erg. *Geol. Soc. Am. Abstr. Programs* 44 (6), 80.
- Ransome, F.L., 1903. Geology of the Globe Copper District, Arizona: U.S. Geological Survey Professional Paper 12, 168 p., 2 sheets, scales 1:62,500, and 1:12,000.
- Reader, John, 2001. In: Africa: National Geographic Society, Washington, D.C., pp. 227–228.
- Reynolds, S.J., Bartlett, R.D., 2002. Subsurface geology of the easternmost Phoenix basin, Arizona: implications for groundwater flow. *Ariz. Geol. Surv. Contrib. Rep.*, CR-02-A. p. 1–35.
- Reynolds, S.J., Florence, F.P., Welty, J.W., Roddy, M.S., Currier, D.A., Anderson, A.V., Keith, S.B., 1986. Compilation of radiometric age determinations in Arizona. *Ariz. Bureau Geol. Miner. Tech. Geol. Surv. Branch Bull.* 197.
- Richard, S.M., Reynolds, S.J., Spencer, J.E., Pearthree, P.A., 2000. *Geologic Map of Arizona*. Arizona Geological Survey Map [M.S. thesis], 35, 319 p.
- Richard, S.M., Spencer, J.E., 1998. Compilation geologic map of the Ray - Superior area, Central Arizona. *Ariz. Geol. Surv. Open File Rep.* 98-13.
- Scarborough, R.B., 1989. Cenozoic erosion and sedimentation in Arizona. In: Jenney, J.P., Reynolds, S.J. (Eds.), *Geologic evolution of Arizona: Arizona Geological Society Digest*, 17, pp. 515–537.
- Scarborough, R.B., 2001. Neogene development of the Little Colorado River valley and eastern Grand Canyon: field evidence for an overtopping hypothesis. In: Young, R.A., Spamer, E.E. (Eds.), *Colorado River Origin and Evolution, Grand Canyon Association*, Monograph no. 12, pp. 207–214.
- Schrider, A.F., 1967. Younger Precambrian geology in southern Arizona. *U.S. Geol. Surv. Prof. Pap.* 566.
- Skotnicki, S.J., 2002. *Geologic map of the Sierra Ancha, central Arizona*. In: *Arizona Geological Survey Digital Geologic Map 24 (2 Sheets)*.
- Skotnicki, S.J., DePonty, J.D., 2020. Subsurface evidence for the sudden integration of the Salt River across the internally drained Basin and Range Province, Arizona, USA. *Geomorphology* 371. <https://doi.org/10.1016/j.geomorph.2020.107429>.
- Sears, J.W., 2013. Late Oligocene-Early Miocene Grand Canyon: a Canadian connection? *GSA Today* 23 (11), 4–10. <https://doi.org/10.1130/GSATG178A.1>.
- Sirrine, G.K., 1958. *Geology of the Springerville - St. Johns Area, Apache County, Arizona* [Ph.D. thesis]. University of Texas, Austin, 247 p.
- Skotnicki, S.J., Seong, Y.B., Dorn, R.I., Larson, P.H., DePonty, J., Jeong, A., 2020. Drainage integration of the Salt and Verde rivers in a Basin and Range extensional landscape, Central Arizona, USA. *Geomorphology* 374. <https://doi.org/10.1016/j.geomorph.2020.107512>.
- Spencer, J.E., Reynolds, S.J., 1989. Middle Cenozoic tectonics of Arizona and adjacent areas. In: Jenney, J.P., Reynolds, S.J. (Eds.), *Geologic Evolution of Arizona: Arizona Geological Society Digest*, 17, pp. 539–574.
- Thompson, K.S., Potochnik, A.R., Ryel, R., O'Brien, G., Neal, L.A., 2000. Development of a geomorphic model to predict erosion of pre-dam Colorado River terraces

- containing archaeological resources. In: SWCA Environmental Consultants, Inc., Submitted to Grand Canyon Monitoring and Research Center, Flagstaff, AZ, 130 p., 6 plates.
- Witcher, J.C., Hahman, R.W., Swanberg, C.A., 1994. Alpine 1/federal corehole -subsurface stratigraphy of the eastern White Mountains, Apache County, Arizona. In: Chamberlin, R.M., Kues, B.S., Cather, S.M., Barker, J.M., McIntosh, W.C. (Eds.), New Mexico Geological Society 45th Annual Field Conference Guidebook. New Mexico Geological Society, pp. 223–240.
- Wrucke, C.T., 1989. The Middle Proterozoic Apache Group, Troy Quartzite, and associated diabase of Arizona. In: Reynolds, S.J., Jenney, J.P. (Eds.), Geologic Evolution of Arizona, Arizona Geological Society Digest, 17, pp. 239–258.
- Young, R.A., Brennan, W.J., 1974. Peach Springs Tuff; its bearing on structural evolution of the Colorado Plateau and development of Cenozoic drainage in Mohave County, Arizona. *Geol. Soc. Am. Bull.* 85, 83–90.
- Young, R.A., Hartman, J.H., 2011. Early Cenozoic “Rim Gravel” of Arizona—age, distribution and geologic significance. In: Beard, L.S., Karlstrom, K.E., Young, R.A., Billingsley, G.H. (Eds.), CRevolution 2—Origin and Evolution of the Colorado River System, Workshop Abstracts: U.S. Geological Survey Open-File Report 2011–1210, pp. 274–286.
- Zachos, J.C., Dickens, G.R., Zeebe, R.E., 2008. An early Cenozoic perspective on greenhouse warming and carbon-cycle dynamics. *Nature* 451, 279–283.